

MODELING OF HEAT AND MASS TRANSFER IN MICROWAVE-INFRARED
HEATING OF ZUCCHINI

A THESIS SUBMITTED TO
THE GRADUATE SCHOOL OF NATURAL AND APPLIED SCIENCES
OF
MIDDLE EAST TECHNICAL UNIVERSITY

BY

NALAN YAZICIOĞLU

IN PARTIAL FULFILLMENT OF THE REQUIREMENTS
FOR
THE DEGREE OF DOCTOR OF PHILOSOPHY
IN
FOOD ENGINEERING

APRIL 2016

Approval of the thesis:

**MODELING OF HEAT AND MASS TRANSFER IN MICROWAVE-
INFRARED HEATING OF ZUCCHINI**

submitted by **NALAN YAZICIOĞLU** in partial fulfillment of the requirements for
the degree of **Doctor of Philosophy in Food Engineering Department, Middle
East Technical University** by,

Prof. Dr. Gülbin Dural Ünver _____
Graduate School of **Natural and Applied Sciences**

Prof. Dr. Alev Bayındırlı _____
Head of Department, **Food Engineering**

Prof. Dr. Servet Gülüm Şumnu _____
Supervisor, **Food Engineering Dept., METU**

Prof. Dr. Serpil Şahin _____
Co-Supervisor, **Food Engineering Dept., METU**

Examining Committee Members:

Prof. Dr. Ferhunde Us _____
Food Engineering Dept., Hacettepe University

Prof. Dr. Servet Gülüm Şumnu _____
Food Engineering Dept., METU

Prof. Dr. Esra Yener _____
Food Engineering Dept., METU

Assoc. Prof. Dr. İlkay Şensoy _____
Food Engineering Dept., METU

Assist. Prof. Dr. Özge Şakıyan _____
Food Engineering Dept., Ankara University

Date: _____

I hereby declare that all information in this document has been obtained and presented in accordance with academic rules and ethical conduct. I also declare that, as required by these rules and conduct, I have fully cited and referenced all material and results that are not original to this work.

Name, Last name : Nalan YAZICIOĞLU

Signature :

ABSTRACT

MODELING OF HEAT AND MASS TRANSFER IN MICROWAVE- INFRARED HEATING OF ZUCCHINI

Yazıcıođlu, Nalan

Ph.D., Department of Food Engineering

Supervisor : Prof. Dr. Glm Őumnu

Co-Supervisor: Prof. Dr. Serpil Őahin

April 2016, 96 pages

The main objective of this study is to develop a finite element model to predict the variation of temperature and moisture content of zucchini during microwave-infrared heating. There is no information in literature about heating of zucchini by using this method. Heat and mass transfer in zucchini heated in microwave and infrared combination oven were modelled by Finite Element method. Microwave power was predicted by using the exact form of Lambert Law and calculating the electric field distribution by Maxwell Equations. Measured temperature at different positions of zucchini and moisture content data were used to verify the models obtained for different microwave and infrared powers. Models based on Lambert Law were determined for the combination of 10, 30 and 50% microwave and 10, 40 and 70% infrared powers for 600 s. These models were in good agreement with the experimental data with an average root mean square error (RMSE) of 5.66 for temperature and 2.52 for moisture content. Microwave power dependency of incident surface power and moisture diffusivity and microwave and infrared power dependency of mass transfer coefficient, which were determined in

modeling based on Lambert Law, were empirically modelled. Models based on Maxwell Equations were determined for the combination of 10% microwave and 10, 40 and 70% infrared powers for 100 s. Models fitted well with an average RMSE of 4.15 for temperature and 0.39 for moisture content. Generally, models derived from the Maxwell Equations gave better results of temperature and moisture content than models developed by Lambert Law.

Keywords: Modeling, microwave, infrared, Lambert Law, Maxwell Equations

ÖZ

KABAĞIN MİKRODALGA-KIZILOTESİ İLE ISITILMASINDA ISI VE KÜTLE TRANSFERİNİN MODELLEMESİ

Yazıcıoğlu, Nalan

Doktora, Gıda Mühendisliği Bölümü

Tez Yöneticisi : Prof. Dr. Gülüm Şumnu

Ortak Tez Yöneticisi: Prof. Dr. Serpil Şahin

Nisan 2016, 96 sayfa

Bu çalışmanın ana amacı, kabağın mikrodalga-kızılötesi ile ısıtılması sırasında kabağın ısı ve kütle değişimini tahmin etmek için sonlu eleman modelinin oluşturulmasıdır. Bu metodu kullanarak kabağın ısıtılması hakkında literatürde bilgi bulunmamaktadır. Mikrodalga-kızılötesi kombinasyonlu fırında ısıtılmış kabağın ısıtılması sırasında ve kütle transferi Sonlu Eleman metodu ile modellenmiştir. Mikrodalga gücü Lambert Kanununun kesin formatı kullanılarak ve Maxwell Denklemleri ile elektrik alan hesaplanarak tahmin edilmiştir. Kabağın farklı noktalarında ölçülen sıcaklık ve nem içeriği verileri, farklı mikrodalga ve kızılötesi güçler için elde edilen modellerin doğrulanmasında kullanılmıştır. Lambert Kanunu kaynaklı modeller 600 sn için % 10, 30 ve 50 mikrodalga ve % 10, 40 ve 70 kızılötesi güçlerinin kombinasyonu için belirlenmiştir. Modeller deneysel verilere uygunluk göstermiştir ki ortalama hatanın karesinin kökü sıcaklık için 5.66, nem miktarı için 2.52'dir. Lambert Kanunu kaynaklı modellerde elde edilen, yüzey gücü ve nem difüzyon katsayısının mikrodalga gücüne ve kütle transferi katsayısının mikrodalga ve kızılötesi gücüne bağımlılığı empirik olarak

modellenmiştir. Maxwell Denklemleri kaynaklı modeller 100 sn için %10 mikrodalga ve %10, 40 ve 70 kızılötesi güçlerinin kombinasyonu için belirlenmiştir. Modeller deneysel verilere uygunluk göstermiştir ki ortalama hatanın karesinin kökü sıcaklık için 4.15, nem miktarı için 0.39'dur. Genel olarak, Maxwell Denklemleri kaynaklı modeller Lambert Kanunu ile oluşturulan modellerden daha iyi ısı ve nem miktarı sonuçları vermiştir.

Anahtar Kelimeler: modelleme, mikrodalga, kızılötesi, Lambert Kanunu, Maxwell Denklemleri

Dedicated to Mustafa Bera YAZICIOĞLU...

ACKNOWLEDGEMENTS

I wish to express my sincere gratitude and respect to my supervisor Prof. Dr. Gülüm Şumnu and my co-supervisor Prof. Dr. Serpil Şahin for their continuous support, encouragement, and valuable suggestions in every step of my study.

I would like to thank President of TAPDK, Suat Evcimen, head of my department Hüseyin Ürnez, my friends at work, Nazım, Ayşe Gökalp, Devlet, Hatice, Hasan, Banu, Özge, Gülsevil for their support.

I do not have words to explain how to express my thanks and my deepest gratitude to my family for their love, support and encouragement. During my study they looked after my son and even me. This study would not be able to come up if they were not around helping me in every possible way. I am definitely dedicating this study to my family: Mustafa Sait Yazicioğlu, Asiye Yazicioğlu, Beduh Uysal, Seher Uysal, Halil Uysal and Nevra Yazicioğlu.

My very special thanks go to my husband Faruk Yazıcıoğlu for his precious support and endless love in my life. I am very grateful to him for his patience and endless support in every step of my education. Words are incapable to express my appreciation to him.

TABLE OF CONTENTS

ABSTRACT	v
ÖZ.....	vii
ACKNOWLEDGEMENTS	x
TABLE OF CONTENTS	xi
LIST OF TABLES	xiv
LIST OF FIGURES	xv
CHAPTERS	
1.INTRODUCTION.....	1
1.1 Microwave Heating	1
1.2 Infrared Heating.....	3
1.3 Microwave- Infrared Combination Heating	4
1.4 Modeling of Heat and Mass Transfer in Microwave Processing	5
1.5 Modeling of Heat and Mass Transfer in Infrared Processing.....	8
1.6 Modeling of Heat and Mass Transfer in Microwave-Infrared Combination Processing	9
1.7 Aim of Study	10
2. MODEL DEVELOPMENT	13
2.1 Mathematical Formulation of Microwave Heating	13
2.1.1 Determination of Electric Field by Maxwell Equations.....	15
2.1.2 Determination of Microwave Power by Lambert Law.....	18
2.2 Mathematical Formulation of Infrared Heating.....	22
2.3 Numerical Solution.....	22

3. MATERIALS AND METHODS	25
3.1 Sample Preparation and Microwave Infrared Combination Heating	25
3.2 Measurement of Temperature	26
3.3 Measurement of Moisture Content	28
3.4 Measurement of Density	28
3.5 Thermal Conductivity	29
3.6 Specific Heat Capacity	29
3.7 Dielectric Properties	29
3.8 Heat Transfer Coefficient	29
3.9 Modeling and Data Analysis	30
3.10 Modeling by Lambert Law	30
3.10.1 Parameters Used for Modeling by Lambert Law	31
3.10.2 Mesh Properties for Modeling by Lambert Law	32
3.10.3 Infrared Boundary Condition for Modeling by Lambert Law	34
3.10.4 Heat Flux Boundary Condition for Modeling by Lambert Law	34
3.10.5 Mass transfer model setup for Modeling by Maxwell Equations	34
3.11 Modeling by Maxwell Equations	34
3.11.1 Parameters Used for Modeling by Maxwell Equations	35
3.11.2 Explicit Selections for Modeling by Maxwell Equations	37
3.11.3 Material Properties for Modeling by Maxwell Equations	38
3.11.4 Mesh Properties for Modeling by Maxwell Equations	38
3.11.5 Microwave Heating Model Setup for Modeling by Maxwell Equations ..	40
3.11.6 Infrared Boundary Condition for Modeling by Maxwell Equations	42
3.11.7 Heat Flux Boundary Condition for Modeling by Maxwell Equations	42
3.11.8 Mass Transfer Model Setup for Modeling by Maxwell Equations	42
4. RESULTS AND DISCUSSION	43

4.1 Experimental and Model Results Based on Lambert Law	44
4.2 Empirical Modeling of Parameters Obtained for Models Based on Lambert Law	55
4.3 Experimental and Model Results Based on Maxwell Equations.....	56
4.4 Effect of Microwave and Infrared Powers on Temperature Distribution and Moisture content of Zucchini	62
4.4.1 Effect of Microwave Power on Temperature and Moisture content of Zucchini	63
4.4.2 Effect of Infrared Power on Temperature and Moisture content of Zucchini	67
4.4.3 Variation of Temperature with Respect to Position in Zucchini	71
4.4.4 Variation of Moisture Content with Respect to Position in Zucchini.....	73
4.5 Comparison of Models Based on Maxwell Equations and Lambert Law	74
5. CONCLUSION AND RECOMMENDATIONS	81
REFERENCES	83
CURRICULUM VITAE	95

LIST OF TABLES

TABLES

Table 3.1 Positions of temperature probes	28
Table 3.2 Parameters used for the simulation done by Lambert Law	31
Table 3.3 Mesh properties	33
Table 3.4 Mesh size.....	33
Table 3.5 Parameters used for the simulation done by Maxwell Equations	36
Table 3.6 Properties of air, silicon carbide (porcelain) and structural steel.....	38
Table 3.7 Mesh properties	39
Table 3.8 Mesh size.....	39
Table 4.1 Parameter values obtained for models based on Lambert Law for different microwave and infrared power operating conditions.....	46
Table 4.2 Root mean square errors (RMSE) calculated by experimental data and models obtained based on Lambert Law for temperature at different positions of zucchini and moisture content.....	46
Table 4.3 Empirical models for parameters	56
Table 4.4 Parameter values obtained for models based on Maxwell Equations for different microwave and infrared power operating conditions	58
Table 4.5 Root mean square errors (RMSE) calculated by experimental data and models obtained based on Maxwell Equations for temperature at different positions of zucchini and moisture content.....	58
Table 4.6 Root Mean Square Errors (RMSE) of Lambert and Maxwell models obtained for different microwave (MWP) and infrared powers (IRP) and positions of the temperature probe.....	78
Table 4.7 Root Mean Square Errors (RMSE) of Lambert and Maxwell models obtained for moisture content predictions for different microwave (MWP) and infrared powers (IRP).....	78

LIST OF FIGURES

FIGURES

Figure 3.1 Schematic diagram of microwave–infrared combination oven.	26
Figure 3.2 Position of temperature probes in the zucchini	27
Figure 3.3 Sensitive zone of the temperature probe.....	28
Figure 3.4 Sketch of 2D axisymmetric rectangular model of zucchini.....	32
Figure 3.5 Meshed 2D axisymmetric rectangular model of zucchini	33
Figure 3.6 Sketch used for modeling of the entire oven together with rectangular waveguide and zucchini	37
Figure 3.7 Sketch used for modeling of the zucchini.....	37
Figure 3.8 Sketch of meshed oven	39
Figure 3.9 Sketch of port boundary.....	40
Figure 3.10 Sketch of metal boundaries.....	41
Figure 3.11 Sketch of symmetry boundary	41
Figure 4.1 Lambert model (line) and experimental (dotted line) results of temperature at (a) $r=10.5$ mm, (b) $r=0.0$ and (c) $r=6.1$ mm and (d) moisture content of zucchini heated by 10% microwave and 10% upper infrared power.....	47
Figure 4.2 Lambert model (line) and experimental (dotted line) results of temperature at (a) $r=10.5$ mm, (b) $r=0.0$ and (c) $r=6.1$ mm and (d) moisture content of zucchini heated by 10% microwave and 40% upper infrared power.....	48
Figure 4.3 Lambert model (line) and experimental (dotted line) results of temperature at (a) $r=10.5$ mm, (b) $r=0.0$ and (c) $r=6.1$ mm and (d) moisture content of zucchini heated by 10% microwave and 70% upper infrared power.....	49
Figure 4.4 Lambert model (line) and experimental (dotted line) results of temperature at (a) $r=10.5$ mm, (b) $r=0.0$ and (c) $r=6.1$ mm and (d) moisture content of zucchini heated by 30% microwave and 10% upper infrared power.....	50

Figure 4.5 Lambert model (line) and experimental (dotted line) results of temperature at (a) $r=10.5$ mm, (b) $r=0.0$ and (c) $r=6.1$ mm and (d) moisture content of zucchini heated by 30% microwave and 40% upper infrared power.....	51
Figure 4.6 Lambert model (line) and experimental (dotted line) results of temperature at (a) $r=10.5$ mm, (b) $r=0.0$ and (c) $r=6.1$ mm and (d) moisture content of zucchini heated by 30% microwave and 70% upper infrared power.....	52
Figure 4.7 Lambert model (line) and experimental (dotted line) results of temperature at (a) $r=10.5$ mm, (b) $r=0.0$ and (c) $r=6.1$ mm and (d) moisture content of zucchini heated by 50% microwave and 10% upper infrared power.....	53
Figure 4.8 Lambert model (line) and experimental (dotted line) results of temperature at (a) $r=10.5$ mm, (b) $r=0.0$ and (c) $r=6.1$ mm and (d) moisture content of zucchini heated by 50% microwave and 40% upper infrared power.....	54
Figure 4.9 Lambert model (line) and experimental (dotted line) results of temperature at (a) $r=6.1$ mm, (b) $r=0.0$ and (c) $r=10.5$ mm and (d) moisture content of zucchini heated by 50% microwave and 70% upper infrared power.....	55
Figure 4.10 Maxwell model (line) and experimental (dotted line) results of temperature at (a) $r=10.5$ mm, (b) $r=0.0$ and (c) $r=6.1$ mm and (d) moisture content of zucchini heated by 10% microwave and 10% upper infrared power.....	59
Figure 4.11 Maxwell model (line) and experimental (dotted line) results of temperature at (a) $r=10.5$ mm, (b) $r=0.0$ and (c) $r=6.1$ mm and (d) moisture content of zucchini heated by 10% microwave and 40% upper infrared power.....	60
Figure 4.12 Maxwell model (line) and experimental (dotted line) results of temperature at (a) $r=10.5$ mm, (b) $r=0.0$ and (c) $r=6.1$ mm and (d) moisture content of zucchini heated by 10% microwave and 70% upper infrared power.....	61
Figure 4.13 Electric field (V/m) at $z=0.08$ cm and the surface temperature of the zucchini of the zucchini at $t=100$ s.....	62
Figure 4.14 Lambert model (line) and experimental (dotted line) results of temperature at the center ($r=0.0$) of the zucchini heated by 10% infrared and 50% microwave (black) and 10% infrared and 10% microwave power (gray)	64
Figure 4.15 Lambert model (line) and experimental (dotted line) results of temperature at the center ($r=0.0$) of the zucchini heated by 70% infrared and 50% microwave (black) and 70% infrared and 10% microwave power (gray)	64

Figure 4.16 Lambert model (line) and experimental (dotted line) results of temperature at the center ($r=0.0$) of the zucchini heated by 10% infrared and 50% microwave (black) and 10% infrared and 30% microwave power (gray)	65
Figure 4.17 Lambert model (line) and experimental (dotted line) results of moisture content of the zucchini heated by 10% infrared and 50% microwave (gray) and 10% infrared and 10% microwave power (black)	66
Figure 4.18 Lambert model (line) and experimental (dotted line) results of moisture content of the zucchini heated by 70% infrared and 50% microwave (gray) and 70% infrared and 10% microwave power (black)	67
Figure 4.19 Lambert model (line) and experimental (dotted line) results of temperature at $r=10.5$ mm of the zucchini heated by 70% infrared power and 10% microwave power (black) and 10% infrared power and 10% microwave power (gray)	68
Figure 4.20 Lambert model (line) and experimental (dotted line) results of temperature at $r=10.5$ mm of the zucchini heated by 70% infrared power and 30% microwave power (black) and 10% infrared power and 30% microwave power (gray)	69
Figure 4.21 Lambert model (line) and experimental (dotted line) results of temperature at $r=10.5$ of the zucchini heated by 40% infrared power and 50% microwave power (black) and 10% infrared power and 50% microwave power (gray)	69
Figure 4.22 Lambert model (line) and experimental (dotted line) results of moisture content of the zucchini heated by 70% infrared power and 10% microwave power (gray) and 10% infrared power and 10% microwave power (black)	70
Figure 4.23 Lambert model (line) and experimental (dotted line) results of moisture content of the zucchini heated by 70% infrared power and 30% microwave power (gray) and 10% infrared power and 30% microwave power (black)	71
Figure 4.24 Lambert model (line) and experimental (dotted line) results of temperature of the zucchini heated by 10% infrared and 10% microwave power at $r=0.0$ (black) and $r=10.5$ mm (gray)	72

Figure 4.25 Lambert model (line) and experimental (dotted line) results of temperature of the zucchini heated by 40% infrared power and 10% microwave power at $r=0.0$ (black) and $r=6.1$ (gray) 73

Figure 4.26 Simulation moisture content data when (a) 70% infrared and 50% microwave, (b) 70% infrared and 10% microwave power were selected for 600 s heating time. 74

Figure 4.27 Maxwell Model (black line), Lambert Model (gray line) and experimental (dotted line) results of temperature at (a) $r=10.5$ mm, (b) $r=0.0$ and (c) $r=6.1$ mm (surface) of the zucchini and (d) moisture content of zucchini heated by 10% microwave power and 10% upper infrared power for 100 s. 75

Figure 4.28 Maxwell Model (black line), Lambert Model (gray line) and experimental (dotted line) results of temperature at (a) $r=10.5$ mm, (b) $r=0.0$ and (c) $r=6.1$ mm (surface) probes of the zucchini and (d) moisture content of zucchini heated by 10% microwave power and 40% upper infrared power for 100 s. 76

Figure 4.29 Maxwell Model (black line), Lambert Model (gray line) and experimental (dotted line) results of temperature at (a) $r=10.5$ mm, (b) $r=0.0$ and (c) $r=6.1$ mm (surface) probes of the zucchini and (d) moisture content of zucchini heated by 10% microwave power and 70% upper infrared power for 100 s. 77

CHAPTER 1

INTRODUCTION

1.1 Microwave Heating

Microwaves are electromagnetic waves of energy having wavelength between radio and infrared waves on the electromagnetic spectrum with frequencies between 300 MHz and 30 GHz (Giese, 1992). Microwaves are usually generated by “magnetron” an electromagnetic device. Microwaves radiate outward from this source and can be absorbed, transmitted, and reflected by the food (Giese, 1992). Ohlsson and Bengtsson, (2002) stated that in food industry, frequencies of either 2450 MHz or 915 MHz are used which corresponds to 12 cm or 34 cm in wavelength, respectively.

The main property of the microwave heating is that heat is generated throughout the food. However, in conventional heating, heat is transferred from the surface to the inner parts of the food. In microwave heating, because of the low air temperature in the microwave oven and the cooling effects of evaporation, the interior temperature of food is hotter than the surface temperature (Decareau, 1992). Therefore, microwave heating leads to fast heating and shorter processing times with respect to conventional heating.

There are two microwave heating mechanisms which are ionic conduction and dipolar rotation. Polar solvents give rise to dipolar rotation in the presence of electric field and the rotation causes molecular friction. The energy resulted from the friction penetrates into food and generates volumetric heating. Electric field moves the charged molecules in a way that as one molecule moves in one direction, the opposite charged molecule moves in the other direction. This vibration causes kinetic energy and volumetric heating of food (Decareau, 1992; Sahin & Sumnu, 2006).

Alton, 1998 stated that the dipolar rotation and ionic conduction were caused by changes of the magnetic and electrical fields through the food.

Microwave heating was generally applied to dry food materials. The aim of drying of foods is to dry foods without altering their physical and chemical quality. Because of its higher rate of moisture removal and shorter cooking time, microwave heating leads to less change in physical and chemical properties of food. Moisture in food absorbs the penetrated microwaves directly. This creates an outward flux of quickly removing vapor transfer and rapid evaporation of water (Feng et al., 2001). Shrinkage has been a common problem in conventional heating methods. Shrinkage in conventional heating can be solved by microwave drying since this rapid outward flow prevents the texture to collapse or shrink. Because of these unique advantages, in recent years, microwave heating has gained importance as an alternative method to dry for a variety of food products such as snack foods, dairy products, fruits and vegetables.

In literature, microwave heating was applied to a number of products such as for plain yogurt (Kim and Bhowmik, 1995), skimmed milk, whole milk, casein powders, butter, fresh pasta (Al-Duri and McIntyre, 1992), cranberries (Yongsawatdigul and Gunasekaran 1996), carrot slices (Lin et al., 1998), model fruit gels (Drouzas and Saravacos, 1999), pea (Kadlec et al., 2001), macadamia nuts (Silva et al., 2006), apple (Bilbao-Sainz et al., 2006), grapes (Tulasidas et al., 1996), potato slices (Bouraout et al., 1994), apple and mushroom (Funebo and Ohlsson, 1998), American ginseng roots (Ren and Chen, 1998), peach (Wang and Sheng, 2006), and blueberries (Feng et al. 2000).

Microwave heating may cause excessive temperature rise along the corner or edges of food products which results in burns and production of undesirable flavors. To prevent these unwanted circumstances and to understand the heating and moisture removal ability of microwave infrared combination oven better, heat and mass transfer during microwave heating should be analyzed.

1.2 Infrared Heating

Infrared is invisible radiant energy present between the spectrums of ultraviolet and microwave in the electromagnetic spectrum (Sepulveda and Barbosa-Canovas, 2003). Infrared radiation is situated in the sun's electromagnetic spectrum that is overwhelmingly responsible for the heating property of the sun (Ranjan and Irudayaraj, 2002).

Infrared radiation mechanism includes a heat source (radiator or emitter) and a reflector. Radiator can be heated electrically or by gas fire. Halogen lamp which emits infrared radiation in different wavelengths is the most commonly used infrared source since 1984. Halogen lamp provides near-infrared radiation energy, which has lower penetration depth and higher frequency than the other infrared sources. The most known advantage of infrared heating is the rapid surface heating since the penetration of infrared radiation is poor. After the halogen lamp emits infrared radiation, food absorbs the energy through conduction and convection (Sepulveda and Barbosa-Canovas, 2003). The generated heat is transferred from the surface of the food to the center of the food, thus mass is transported from the center to the surface of the food. (Jaturonglumlert and Kiatsiriroat, 2010). For infrared heating there is no need for a medium to transfer energy from source to food.

Each food absorbs the energy coming from halogen lamp in a different amount. The emitted energy amount can be affected by some factors such as thickness of the food (Land, 2012). High moist foods can penetrate the radiation energy whereas solid foods absorb the energy in a thin layer at the surface. Penetration rate depends on the moisture content of the food (Lampinen et al., 1991). Moreover, during the drying process moisture content decreases which changes the radiation features of the food. The wavelength is also a factor for radiation penetration. As wavelength increases, infrared radiation is focused more on the surface, and at short wavelengths it can penetrate through the food. Therefore, for thick layer foods, far infrared radiation is effective while for thinner foods, near infrared radiation is effective (Nowak and Levicki, 2004).

Moreover, Datta and Ni (2002) stated that the surface temperature increases as the infrared radiation penetration depth decreases. The increase in surface temperature increases surface moisture loss. Thus, infrared heating can be recommended as a drying method.

In literature, infrared was applied on food products such as potatoes (Afzal and Abe, 1998), apples (Nowak and Levicki, 2004; Togrul 2005), sweet potatoes (Sawai et al., 2004), onions (Mongpreneet et al., 2002; Sharma et al., 2005) and kiwifruit (Fenton and Kennedy, 1998). Dostie et al. (1989), Masamura et al. (1988), Wang and Sheng (2004) also used infrared energy on foods. Dostie et al. (1989), found that in the presence of infrared drying time was to 2-2.5 times less as compared to convective drying. Masamura et al. (1988), dried potato using infrared heater and found that when the electric power supplied to the far infrared heater increased, the rate of drying increased. Onion slices were heated by infrared radiation and the time of drying was found to be 2.25 times less when power increased from 300 to 500 W (Sharma et al., 2005). It was concluded that quality of carrots dried by infrared radiation and freeze drying were similar (Namiki et al., 1996). When apple slices were dried by infrared radiation and convective drying, it was found that the time of drying was decreased to 50% in the presence of infrared drying (Nowak and Levicki 2004).

1.3 Microwave- Infrared Combination Heating

Microwave-infrared combination heating combines two heating mechanisms which are microwave heating and infrared heating. In microwave heating, the food is heated volumetrically and moisture moves from the inside of the food to the surface and accumulates there. However, by infrared heating, food is heated from the surface. By combination heating, moisture accumulation on the surface of the food which is the main disadvantage of microwave heating, can be avoided by surface moisture removal property of infrared.

Almeida (2005), stated that in combination heating, the main temperature rise was approximately the sum of microwave and infrared heating since these mechanisms were independent, additive and changing only the final temperature distribution. It

was concluded that combination heating was considerably faster, leading to higher variation in temperatures.

In literature, Sumnu et al. (2005) dried carrot slices by using microwave and microwave-infrared combination oven. These drying methods were compared in terms of colour of the carrots, drying time and rehydration capacity. It was found that microwave-infrared combination drying reduced the drying time 98% as compared to conventional drying, and concluded that microwave-infrared combination drying gave a higher-quality product.

Peach was dried by Wang and Sheng (2006) by using far-infrared heating combined with microwave heating. Khir et al (2011), dried rough rice using microwave-infrared combination system and suggested that microwave energy could be used for the initial stage of moisture removal since at the beginning, food had high moisture content.

Tireki et al. (2006a) used infrared-assisted microwave drying for production of bread crumbs and determined drying conditions in infrared-microwave oven to produce the highest quality bread crumbs. In the study, drying time was 96.8–98.6% less than the conventional drying and bread crumbs dried in combination oven were found to be comparable in terms of color and water binding capacity.

Aydogdu et al. (2015) dried eggplant by using microwave infrared combination oven and conventional hot air tray dryer. It was concluded that drying time was decreased significantly when microwave and infrared powers increased. Moreover, eggplants dried in combination oven had more porous structure, lower shrinkage and higher rehydration than hot-air-dried ones. Thus, they recommended microwave infrared combination method for drying of eggplants.

1.4 Modeling of Heat and Mass Transfer in Microwave Processing

Mathematical modeling of a system can be used to optimize the system operators to predict the hot and cold with dry and moist points, to examine the microbial and nutritional change and to analyze heating techniques for food quality and safety.

Ohlsson and Bengtsson (1971) studied modeling of infinite slabs of salted ham and beef heated by the microwave. Temperature profiles of the model were compared with the experimental results and they were found to be comparable. By then, microwave heating was modeled by several researchers. Swami (1982) modeled cylindrical and rectangular shaped high moisture gel samples. Tong (1988) and Wei et al. (1985) modeled heat and mass transfer of bread, biscuit, muffin and sandstone using one dimensional finite difference. Lin et al. (1995) used TMODEPEP commercial software finite element method which had several advantages over finite difference to demonstrate temperature distribution in agar gels. Chen et al. (1990) added heat generation term to finite element model to analyze temperature profile of a cylinder-shaped potato slice. Ayappa et al. (1991) used Maxwell's equations to describe electromagnetic field distribution. Datta (1990) stated that it would be too difficult to model a rotating food in microwave oven mathematically.

The effect of geometric shape and applied power were systematically studied for model foods (Chamchong and Datta, 1999a; 1999b). Ni et al. (1999) showed that the moisture loss resulted from evaporation and related evaporation to heating uniformity. In this study, authors concluded that when the surface area increased for a given volume, the uniformity of heating increased but the total moisture loss reduced. Finite element based ANSYS software was primarily used in their study.

Pitchai et al. (2012) coupled electromagnetic and heat transfer model for microwave heating in domestic ovens. They developed a comprehensive model to solve coupled electromagnetic and heat transfer equations using finite-difference based commercial software QuickWave v7.5. Validation of the model for 30 s for a cylindrical model food (1% gellan gel) in a 700W microwave oven was developed.

Zhou et al. (1995), applied three-dimensional finite element model (FEM) to predict temperature and moisture distributions in potato during microwave heating using commercial software (TMODEPEP, ANSYS) and predictions were comparable with analytical solutions.

Datta (2007b) provided porous media approaches to study simultaneous heat and mass transfer for microwave heating of foods. Model for small and large pores and generalization of the Darcy's law for flow through a porous medium to Navier–Stokes were developed. Datta (2007a) published the input parameters to the models and demonstrated the application of the models for small pores to convective heating, frying, baking (with and without volume change) and microwave heating.

Microwave heating composes of a complex coupling of electromagnetics and heat and mass transfer. Some assumptions were made for modeling microwave heating such as one directional heating and using Lambert's Law (Von Hippel, 1954; Wei et al., 1985, Mudgett, 1986) instead of Maxwell's equation (Ayappa et al., 1991). Lambert Law gives the power by exponential decay of the energy from the surface to the inner parts of the food (Zhou et al., 1995; Chen et al., 1993; Chamchong and Datta, 1999a, 1999b; Khraisheh et al., 1997; Campanone and Zaritzky, 2005). Ayappa et al. (1991) stated that the exponentially decaying energy assumption for power estimation was only valid for semi-infinite slabs. Critical thickness of the slab above which the Lambert approximation is valid was 2.7 times the penetration depth. However, Lin et al. (1995) obtained the exact form of microwave power term both in cylindrical and rectangular coordinates by the shell balance method. Zhou et al. (1995) concluded that the Lambert's law can be correctly used for cylindrical domain by rewriting the power term by taking the decreasing control volume into account. Power in this case was concentrated along the central axis.

It has been concluded that Lambert's law gives comparable results with the experimental methods numerically (Liu et al., 2005). However, it is not a good way of representing exact microwave power distribution. According to Datta and Anantheswaran (2001), Lambert's Law does not show the exact electromagnetic field. In literature, the Maxwell's and Lambert's Law were compared by several studies to predict temperature of model food in microwave heating (Yang and Gunasekaran, 2004, Liu et al., 2005). Yang and Gunasekaran (2004) stated that using Maxwell's equations was more accurate than Lambert's Law to predict electromagnetic distribution.

1.5 Modeling of Heat and Mass Transfer in Infrared Processing

There is limited literature about the mathematical modeling of heat and mass transfer of infrared heating of foods. The clutter of optical characteristics of food, combination of conduction and convection for transport properties and less radiative energy sources make the research on modeling of heat and mass transfer necessary.

Ratti and Mujumdar (2007) expressed the distribution of infrared radiation which may be absorbed and converted to energy, or reflected from the surface or transmitted by the equation:

$$\rho + \alpha + \tau = 1 \quad (1.1)$$

where, ρ is the reflectivity, α is the absorptivity and τ is the transmissivity. If a body absorbs the entire radiation energy, it is called “black body” ($\alpha = 1$). For black bodies, the emissive power distribution in transparent medium with index n can be expressed with Planck’s law of radiation shown (Jun et al., 2011):

$$E_{b\lambda}(T, \lambda) = \frac{2\pi hc_o^2}{n^2 \lambda^2 \left[e^{\frac{hc_o}{n\lambda kT}} - 1 \right]} \quad (1.2)$$

Where E is emissive power (W/m^2), n is the refractive index of medium, k is known as Boltzmann’s constant ($1.3806 \times 10^{-23} \text{ J/K}$), λ is the wavelength (μm), h is Planck’s constant ($6.626 \times 10^{-34} \text{ J.s}$), T is the source temperature (K) and c_o is the speed of light (km/s).

Models representing the heat and mass transfer phenomenon of infrared drying are generally empirical; namely exponential model, Page model, diffusion model of spherical grain shape and approximation of the diffusion models were applied (Abe and Afzal, 1997, Das et al., 2004, Togrul, 2005).

There are a few studies in which mathematical heat and mass transfer equations were considered. Afzal and Abe (1998) explored how the heat transfer inside food systems

under far infrared radiation changed with diffusion characteristics and thickness of slab. It was found that the internal moisture moved through the surface of the food by the radiation energy and its activation energy was inversely proportional to thickness of slab.

Shilton et al. (2002), studied heat and mass transfer of beef patties during far infrared heating numerically. The finite difference model of an infinite slab was calculated during heating by a far-infrared radiation gas catalytic plaque heater whose radiation temperature was 767 K. In this study, it was concluded that for different fat contents in beef patties, the prediction of the model for the diffusion coefficient based on temperature and moisture content, reached a good agreement with the experimental data.

A three dimensional model to describe potatoes in Cartesian coordinates were used to couple heat, moisture transfer, and pressure equations by using a control volume formulation (Ranjan et al., 2002). Radiative source term was added to the model as an exponentially decreasing energy during infrared heating. Authors indicated that the 3-way coupled model results were better than the 2-way coupled ones in predicting temperature and moisture contents. In the study, model data gave good estimations for the experimental ones.

Sakai and Hanzawa (1994) found that infrared energy absorbed mostly by the surface of the food since water on the surface of the food was predominant energy absorber. Energy on the surface could then be transferred by heat conduction in the food. Authors obtained heat transfer equation with boundary conditions based on this assumption and solved them by using Galerkin's finite element method and the measured temperature distribution in samples was in good agreement with model predictions.

1.6 Modeling of Heat and Mass Transfer in Microwave-Infrared Combination Processing

The individual heat and mass transfer models of microwave and infrared have made it easy to model combination heating. Since food is a matrix of different components

such as carbohydrates, water, fat, etc, generally food like gels were used for modeling purposes. Heat transfer within silicon wafers exposed to microwave co-heating was modeled by Mehinger et al. (2000). Microwave radiation was emitted from a cylindrical TE 02 mode gyrotron operated in pulse providing wave radiation at 28 GHz in six steps.

The combination of microwave and convective drying of a hygroscopic porous material, pine wood, were numerically investigated (Turner et al. 1998). Drying equations derived for porous media were solved by using special code.

Salagnac et al. (2004) studied numerical modeling of the hygrothermal behaviour of a rectangular-shaped porous material, cellular concrete, during hot air-microwave and infrared drying. Temperature, moisture content and pressure profiles were obtained by one dimensional physical model in which energy inputs emitted by the electromagnetic radiation calculated by the Lambert law. Comparison of experimental and calculated results showed that the model suits well.

Infrared and hot air assisted microwave heating was modeled by Datta and Ni (2002). Microwave power flux was assumed to decay exponentially with penetration depth. It was concluded that temperature of the surface was increased leading to removal of surface moisture by the help of infrared energy.

Almeida (2005) modeled infrared and microwave-infrared combination heating of potato in an oven quantitatively. A three dimensional model was obtained by using Maxwell equations. Measurement of optical properties, infrared and combined microwave-infrared heat transfer analysis were done.

1.7 Aim of Study

Microwave heating can be a good alternative to conventional heating. It reduces the process time significantly. However, surface sogginess and uneven heating are some problems observed in microwave heating. These problems can be prevented by moisture removal ability of infrared in microwave infrared combination oven. By microwave infrared combination heating, heating time is significantly reduced and

food having comparable quality with conventionally heated ones can be obtained. There is no information in literature about heating of zucchini by using this method.

Modeling heat and mass transfer in foods is a challenging topic among food scientists but generally model food systems are used in literature. Moreover, modeling of heat and mass transfer of foods in microwave-infrared combination oven has not been clearly stated and understood. Thus, the main objective of this study is to develop a finite element model to predict the variation of temperature and moisture in zucchini during microwave-infrared heating. Instead of using a model system, a real food, zucchini was chosen for modeling. Electric field distribution in the oven, temperature distribution and moisture content of zucchini were estimated by describing microwave power term by Maxwell Equations. Lambert Law, a simpler version to predict microwave heating, was used to give approximation of temperature distribution and moisture content of zucchini. Empirical models for parameters obtained in this study were developed for different microwave and infrared powers. Effect of microwave and infrared power on temperature distribution and moisture content of zucchini were analyzed in this study. Furthermore, the variation of temperature and moisture content with respect to position in the zucchini sample was analyzed. Predicted models were fitted to the experimental data. Moreover, the differences in determination of microwave power by Maxwell Equations and Lambert Law were examined.

CHAPTER 2

MODEL DEVELOPMENT

The principles of modeling process are first defining mathematical formulation of the physical system and then solving the system equations by a numerical method.

2.1 Mathematical Formulation of Microwave Heating

Because of non-linear coupled heat and mass transfer equations, the modeling of microwave heating is challenging. Microwave heating leads to volumetric heating of food which results in moisture being pumped out from the inner part of the food to the surface. On the external surface of the food, the evaporation process takes place. In the present work, some assumptions were made to describe combined microwave fields with infrared in cylindrical non-homogeneous food for models based on Lambert and Maxwell Equations.

For both modeling based on Lambert and Maxwell Equations,

- Dielectric properties were taken as constants, since it was assumed that they would not change significantly with respect to temperature and moisture content within the heating period.
- At the surface of the food, it was assumed that both heat and moisture were lost through convection and evaporation. Radiation was not considered since the temperature of the air inside the microwave-infrared combination oven did not change significantly.
- Surface temperature of the halogen lamp was assumed to be 750K, 800K and 850K for 10%, 40% and 70% infrared powers, respectively.

- Surface emissivity of zucchini was assumed to be 0.9. Hellebrand et al. (2001) measured emissivities of some vegetables and fruits and results were between 0.9-0.97.

For modeling based on Maxwell Equations,

- Waveguide was assumed to be rectangular WR-340 waveguide which worked from 2.20 to 3.30 GHz frequency with dimensions assumed as 86.36 mm and 43.18 mm.
- Resistive metal losses were assumed to be small, and it was accounted in the impedance boundary condition.
- Oven was cut into two symmetric parts to make the calculations easy.

Mass and heat transfer equations were express as:

$$\frac{\partial c}{\partial t} = \nabla \cdot (D \nabla c) \quad (2.1)$$

$$C_p \rho \frac{\partial T}{\partial t} = \nabla \cdot (k \nabla T) + Q_{gen} \quad (2.2)$$

Where, c is the concentration of the species (mol/m^3), D denotes the diffusion coefficient (m^2/s), C_p is specific heat capacity ($\text{J/kg}^\circ\text{C}$), T is temperature ($^\circ\text{C}$), ρ is density (kg/m^3), k is thermal conductivity ($\text{W/m}^\circ\text{C}$), Q_{gen} is the volumetric heat generation term (W/m^3). Mass balance equation includes the diffusion transport, taking the interaction between water and air into account.

Initially the material was assumed to be at uniform temperature and moisture content, thus initial conditions for Equations (2.1) and (2.2) can be expressed as follows:

$$\text{@ time } t=0, T = T_0(x, y, z) \quad (2.3)$$

$$\text{@ time } t=0, c = c_0(x, y, z) \quad (2.4)$$

At the line of symmetry (closed boundary), no heat or mass exchange takes place, thus the heat and mass flux are set equal to zero.

$$n \cdot (-D\nabla c) = 0 \quad (2.5)$$

$$n \cdot (-k\nabla T) = 0 \quad (2.6)$$

At the surface, it was assumed that both heat and moisture was lost through convection and evaporation but no radiation took place.

$$n \cdot (D\nabla c) = k_c (c_b - c) \quad (2.7)$$

$$n \cdot (k\nabla T) = h_T (T_{\text{inf}} - T) + n \cdot (D_m \lambda \nabla c) \quad (2.8)$$

The vaporization of water at the zucchini's outer boundary generates a heat flux out. This is represented by heat flux with the term $D_m \lambda \nabla c$ in the boundary conditions for food surface boundary (Chen et al., 1999), where D_m is the diffusion coefficient for evaporative loss (m^2/s), λ is the molar latent heat of vaporization (J/mol), D is the moisture diffusion coefficient in the food (m^2/s), k_c refers to the mass transfer coefficient (m/s), and c_b denotes the outside air (bulk) moisture concentration (mol/m^3), h_T is the heat transfer coefficient ($\text{W}/(\text{m}^2 \cdot \text{K})$), and T_{inf} is the air temperature inside the oven (K).

2.1.1 Determination of Electric Field by Maxwell Equations

For the heat transfer equation, volumetric heat generation (Q_{gen}) term should be calculated. From the Poynting Theorem, heat absorbed by the food per unit time due to the microwaves can be obtained as;

$$Q_{\text{gen}}(x, y, z, t) = 2\pi f \epsilon_0 \epsilon'' |E| \quad (2.9)$$

Where, f is the frequency, ϵ_0 is the dielectric constant of free space (8.854×10^{-12} F/m), ϵ'' is the dielectric loss factor, and E is the electric field (V/m).

In this study, electric field distribution inside the oven was determined. Electromagnetic heating of microwave was described by James Clerk Maxwell in 1873 as a set of four basic equations. Derived equations were in form of differential and integral, the former was used to govern variations of electric and magnetic fields in space and time.

$$\nabla \times E = -j\omega\mu H \quad (2.10)$$

$$\nabla \times H = J = j\omega\epsilon E \quad (2.11)$$

$$\nabla \cdot \epsilon E = q \quad (2.12)$$

$$\nabla \cdot \mu H = 0 \quad (2.13)$$

Where, E is the electric field intensity (V/m), H corresponds to the magnetic field intensity (A/m), J is the current flux (A/m²), ρ is the density of charge (kg/m³), ω is the angular frequency (rad/s), σ is the electric conductivity (S/m), ε is the permittivity (F/m), and μ is the permeability (H/m).

Equation (2.10) is known as Faraday's Law. The law gives the relation between time varying electric field E and magnetic field. According to the Law, the circulation of electric field is determined by the rate of change of magnetic flux through the surface.

Equation (2.11) is known as Ampere's Law, which relates the magnetic field strength H to the total current density J. Both displacement and conduction currents are expressed by J. The circulation of magnetic field strength around a closed system is equal to the net current passing through the surface. Current is surrounded by a magnetic field.

Electric and magnetic fields are completely specified by Gauss's Laws (Equation 2.12), which requires net electric flux equal to the charges contained within the region meaning that net electric flux out of a region is related to the charge contained within it. Equation (2.13) is Gauss's magnetic law, which requires that net magnetic flux out of a region must be zero (Krishnamoorthy, 2011).

When electromagnetics were delivered through a rectangular waveguide with TE_{1,0} wave propagation mode, the electric field was obtained by Equation (2.14) (Malafronte et al., 2012);

$$\nabla \times \mu_r^{-1} (\nabla \times E) - k_0^2 \left(\epsilon_r - \frac{j\sigma}{\omega \epsilon_0} \right) E = 0 \quad (2.14)$$

Where, E is electric field (V/m), μ_r is sample relative permeability (1), ϵ_0 is permittivity of vacuum (F/m), ϵ_r is sample relative permittivity (1), σ is sample electric conductivity (S/m) and ω is angular frequency (rad/s).

In order to solve these equations, initial and boundary conditions were needed. The walls of the oven cavity were assumed as perfect conductors which implied that the tangential electric field component was zero in the equation.

$$n \times E = 0 \quad (2.15)$$

Microwave oven was cut into two symmetric parts so that magnetic field component at this line was zero.

$$n \times H = 0 \quad (2.16)$$

Where, n represents the unit normal vector to the interface, H represents the magnetic field intensity (A/m).

The rectangular waveguide was excited by a transverse electric (TE) wave. TE wave has no electric field component in the direction of propagation. TE₁₀ mode is the only propagation mode for the frequencies between 1.92 GHz and 3.84 GHz. Since frequency of the microwave oven was 2.45 GHz, TE₁₀ propagation mode was selected.

The propagation constant β was determined from the relation:

$$\beta = \frac{2\pi}{c} \sqrt{v^2 - v_c^2} \quad (2.17)$$

Where, c is speed of light, v_c is the cut-off frequency (The waveguide does not operate below the cut-off frequency) and can be calculated for each of the propagation mode as:

$$(v_c)_{mn} = \frac{c}{2} \sqrt{\left(\frac{m}{a}\right)^2 + \left(\frac{n}{b}\right)^2} \quad (2.18)$$

For TE₁₀ mode propagation, $m=1$ and $n=0$, and a and b are the dimensions of rectangular waveguide (Singh and Verma., 2009).

In x , y and z direction, initially, the electric field in the oven was zero.

$$@ t=0, E_x=E_y=E_z=0 \quad (2.19)$$

The electromagnetic field was excited by the port in z direction with Equation (2.20) (Curet et al., 2014)

$$E_{in}(z) = E_0 \cos\left(\frac{\pi y}{a}\right) \quad (2.20)$$

2.1.2 Determination of Microwave Power by Lambert Law

In a dielectric material, absorbed microwave power can be calculated by Lambert's Law which is a more simplified approach than Maxwell Equations in which electric field determination is required. Heat generation is calculated from the penetration depth of the microwaves inside a food material.

$$P_x = P_0 e^{-2\alpha x} \quad (2.21)$$

Where x is the direction of microwave penetration from the surface (m), α is the attenuation constant (m^{-1}) and P_0 is the incident power at the surface (W).

$$\alpha = \frac{\pi \sqrt{2\varepsilon'} \sqrt{\sqrt{1 + \left(\frac{\varepsilon''}{\varepsilon'}\right)^2} - 1}}{\lambda_0} \quad (2.22)$$

where λ_0 is the wavelength in free space, 12.24 cm at 2.45 GHz

Moreover, Datta and Ni (1999), formulated microwave and infrared heating energy flux as exponentially decaying. It leads to the source terms being formulated as:

$$\dot{q}_{micro}(r) = \frac{F_{micro,0}}{\delta_{micro}(r)} e^{\left(-\int_0^r \frac{dr}{\delta_{micro}(r)}\right)} \quad (2.23)$$

$$\dot{q}_{inf\ ra}(r) = \frac{F_{inf\ ra,0}}{\delta_{inf\ ra}(r)} e^{\left(-\frac{r}{\delta_{inf\ ra}(r)}\right)} \quad (2.24)$$

Here r is the radial distance from the surface (m), $F_{micro,0}$ and $F_{infra,0}$ are the microwave and infrared fluxes at the surface (W/m^2), respectively. δ_{micro} , δ_{infra} are the microwave and infrared penetration depths (m), respectively.

Ayappa et al. (1991) stated that the exponentially decaying energy assumption for power estimation was only valid for semi-infinite slabs. Lamberts Law stated that microwave penetration was one dimensional, the energy was normal to the surface and dissipation of the energy was exponential. However, Lin et al. (1995) obtained the exact form of microwave power source term in cylindrical and rectangular coordinates by the shell balance method. Zhou et al. (1995) also used the exact form of microwave power derived by Lin et al. (1995) and concluded that the Lambert's Law could be correctly used for cylindrical domain by rewriting the power term by taking into account the decreasing control volume.

Lin et al. (1995) obtained the exact form of Lambert Law, accordingly;

The incident surface power per unit area was assumed to be uniform and normal to the surface as seen in Equation (2.25)

$$P_c'' = P_0 / (2\pi R(L + R)) \quad (2.25)$$

Where P_0 is surface power (W), R is the radius of the food (m), L is length (m). In the radial direction the total power incident is:

$$P_R = 2\pi R L P_c'' \quad (2.26)$$

When P_0 in equation (2.25) is replaced by P_R and both sides are divided by $2\pi R L$, power per unit area dissipated from the radial direction to the surface of cylinder becomes:

$$P_r'' = \frac{P_R}{2\pi R L} = \frac{2\pi R L P_c'' e^{-2\alpha(R-r)}}{2\pi R L} = P_c'' \left(\frac{R}{r} \right) e^{-2\alpha(R-r)} \quad (2.27)$$

In the axial direction the total power incident at the end of a cylinder is

$$P_{L/2} = \pi R^2 P_c'' \quad (2.28)$$

Therefore, the surface power per unit area dissipating in the axial direction is:

$$P_z'' = \frac{P_{L/2}}{\pi R^2} = \frac{\pi R^2 P_c'' e^{-2\alpha(L/2-z)}}{\pi R^2} = P_c'' e^{-2\alpha(L/2-z)} \quad (2.29)$$

By doing a shell balance on a cylinder, the power absorbed per unit volume by a shell in the radial direction at a distance r is:

$$\frac{\Delta P_r''}{\Delta r} = \frac{P_{r+\Delta r}'' (2\pi(r+\Delta r)\Delta z) - P_r'' (2\pi r\Delta z)}{2\pi r\Delta r\Delta z} \quad (2.30)$$

For the axial direction again by doing shell balance the power absorbed is:

$$\frac{\Delta P_z''}{\Delta z} = \frac{P_{z+\Delta z}''(2\pi r \Delta r) - P_z''(2\pi r \Delta r)}{2\pi r \Delta r \Delta z} \quad (2.31)$$

By adding equations (2.30) and (2.31) the total power absorbed by the shell can be calculated. The total power absorbed by an infinitesimal volume within a cylinder at any r and z location can be expressed by taking limits, as Δr and Δz approach zero, as:

$$P_c'' = \frac{\partial P_r''}{\partial V} = \frac{\partial P_z''}{\partial V} = \frac{\partial(rP_r'')}{r\partial r} + \frac{\partial P_z''}{\partial z} \quad (2.32)$$

Equations (2.33) and (2.34) are obtained upon differentiating equations (2.27) and (2.29):

$$\frac{\partial P_r''}{\partial r} = \frac{-RP_c''}{r^2} e^{-2\alpha(R-r)} + \frac{2\alpha RP_c''}{r} e^{-2\alpha(R-r)} \quad (2.33)$$

$$\frac{\partial P_z''}{\partial z} = 2\alpha P_c'' e^{-2\alpha(L/2-z)} \quad (2.34)$$

When Equations (2.33) and (2.34) are substituted into Equation (2.32), power absorbed per unit volume in a cylinder can be obtained as:

$$\begin{aligned} P_c'' &= \frac{\partial r P_r''}{r \partial r} + \frac{\partial P_z''}{\partial z} = \frac{P_r''}{r} + \frac{\partial P_r''}{\partial r} + \frac{\partial P_z''}{\partial z} \\ &= \frac{2\alpha R P_c''}{r} e^{-2\alpha(R-r)} + 2\alpha P_c'' e^{-2\alpha(L/2-z)} \end{aligned} \quad (2.35)$$

Equation (2.35) gives the power function for microwaves from only one direction into the food sample. When the incident microwaves from the opposite direction are added, the absorbed power density equation for cylinders becomes:

$$\Phi(r, z) = \frac{2\alpha R P_c}{r} \left[e^{-2\alpha(R-r)} + e^{2\alpha(R+r)} \right] + 2\alpha P_c \left[e^{-2\alpha(L/2-z)} + e^{2\alpha(L/2+z)} \right], \quad (2.36)$$

Equation (2.36) was used in this study to predict microwave power density by Lambert Law.

2.2 Mathematical Formulation of Infrared Heating

The infrared heating energy of a food material can be calculated from the Stefan–Boltzmann Law. According to the law, the total energy of a black body radiated per unit surface area across all wavelengths per unit time is in directly proportional with the fourth power of the black body's temperature T.

$$Q = \varepsilon \sigma (T_s^4 - T^4) \quad (2.37)$$

Where, ε is the surface emissivity, σ is the constant of proportionality called Stefan–Boltzmann constant ($=5.670373 \times 10^{-8} \text{ W}/(\text{m}^2\text{K}^4)$) and T_s is the halogen lamp surface temperature (K) and T is the food temperature (K).

2.3 Numerical Solution

In order to understand and predict the future of the system, differential equations under various conditions such as boundary or initial conditions should be solved. It is generally difficult to obtain the exact solution of the differential equations. To solve these equations numerical methods are usually used. Finite difference method and finite element method are the two common methods. In order to select the best suitable method to solve electromagnetic, heat and mass transfer equations, the differences between these two methods should be analyzed.

1. Finite element method can be applied to complicated geometries or boundaries, whereas finite difference method is suitable for rectangular geometries.
2. Solving finite difference method is easier than finite element method.
3. The accuracy of finite element results is higher than the finite difference method, since it gives better approximation between grid points.

Because of these advantages, electric field (Equation 2.9), temperature (Equation 2.2) and concentration profiles (Equation 2.1), with their boundary conditions were calculated simultaneously using Finite Element Method by the help of a finite element software Comsol Multiphysics version 4.3 (Comsol Inc., Burlington, MA, USA).

CHAPTER 3

MATERIALS AND METHODS

In order to solve the mathematical models some input parameters are necessary. Some of these parameters were obtained experimentally, some of them were obtained from the literature and some of them were obtained in this study to fit the experimental data with the model.

3.1 Sample Preparation and Microwave Infrared Combination Heating

Zucchini samples were cut into cylindrical shape with a height of 30 ± 1 mm and a diameter of 32 ± 1 mm by using mold. Initial temperature of the sample was kept constant at room temperature (20°C).

Microwave–infrared combination oven (Advantium Oven™, General Electric Company, Louisville, KY, USA) shown in Figure 3.1 was used in the study. It provides both microwave and infrared heating. The cavity size of Advantium oven was 21 cm in height, 48 cm in length, and 33 cm in width. There are three halogen lamps each having a maximum power of 1500 W. Two of them were located at the top of the oven and one was located under the rotary porcelain table. Temperature and moisture content of zucchini during heating in microwave infrared oven were recorded for different infrared and microwave powers. Microwave and halogen lamp powers could be adjusted from the dials on the front cover of the oven from 10 to 100% which determines the on-off cycle time of the heat source. For the simplicity, only two upper halogen lamps were activated with powers of 10, 40 and 70% and plate was not rotated. Since microwave heating dominates the heating process, 10, 30 and 50% of microwave power levels were selected. Full factorial combination of the powers were studied for modeling by Lambert Law and 10% microwave power and

10, 40 and 70% infrared power were studied for modeling by Maxwell Equations. 600 and 100 seconds of heating process were taken into account for models with Lambert Law and Maxwell Equations, respectively.

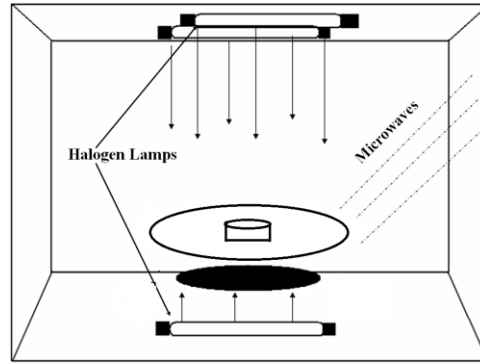


Figure 3.1 Schematic diagram of microwave–infrared combination oven.

In order to predict the actual microwave power in the oven, the maximum power of microwave was determined by IMPI 2-liter test. Two 1 L beakers were used and 1000±5g of water was added in each beaker. The oven was operated at the highest power. Initial water temperature was 20±2 °C. The beakers were placed at the center of the oven side by side in the oven cavity. The oven was operated for 122 s. When the oven was turned off, final water temperature was measured immediately. After three replications, the power was calculated by using Equation (3.1);

$$P(W) = mC_p \frac{\partial T}{\partial t} \quad (3.1)$$

where m is the mass of water (kg), C_p is specific heat capacity (J/kg °C) and T is temperature (°C) and t is time (s) (Buffler, 1993). Maximum microwave power was determined as 618 W.

3.2 Measurement of Temperature

Temperatures were measured with fiber optic temperature probes (FOTL/ 2M, FISO, Canada) at different points of the zucchini. Temperature probes were placed in the

zucchini at three places: center ($r=0.0$), 10.5 mm left side of the center ($r=10.5$ mm) and 6.1 mm right side of the center ($r=6.1$ mm) on the same cross section as shown in Figure 3.2. In Figure 3.3 sensitive zone of the temperature probe was demonstrated. Table 3.1 shows the position of the probes which were determined considering the sensitive zone of the temperature probe. Probes positioned at the left side and the center were placed such that the midpoint temperature of the sample on the vertical axis could be measured. Probe at the right side was placed near the surface to measure surface temperature. After each run, the position of the probes were checked and the ones standing still were considered. Three replications were recorded. Temperatures were recorded in every 0.6 s using a data logger (Agilent 34970A) during the heating process.

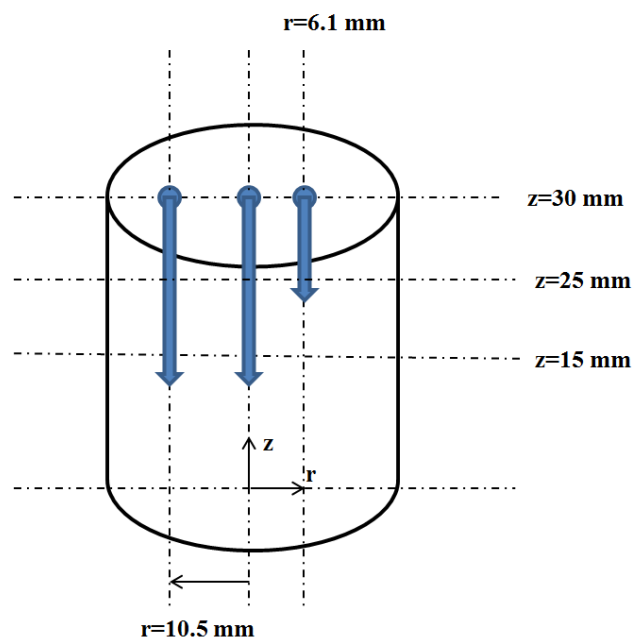


Figure 3.2 Position of temperature probes in the zucchini

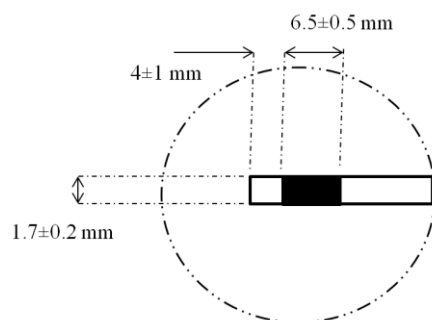


Figure 3.3 Sensitive zone of the temperature probe

Table 3.1 Positions of temperature probes

	r (mm)	z (mm)
Left probe	10.5	11-18
Center probe	0	11-18
Right probe	6.1	25-30

3.3 Measurement of Moisture Content

For moisture content determination, whole zucchini samples were dried in an electrical oven at 105 °C up to the establishment of constant weight (AOAC, 1984). Calculation was done by using weight of the zucchini before it was placed into the oven and weight of the dried zucchini immediately after it was removed from the oven. Moisture content was calculated on wet basis and expressed as percentage (kg water/kg zucchini). Two replications were done. Time of heating was selected as 0, 2, 4, 6, 8 and 10 min.

3.4 Measurement of Density

The volume of the zucchini (V) with a known mass (m) was calculated by the rape seed displacement method (Sahin and Sumnu, 2006) to calculate the density of zucchini.

3.5 Thermal Conductivity

For the thermal conductivity of zucchini, the equation obtained by Ali et al. (2002) was used;

$$k(T, M) = -30.87 \times 10^{-2} + 35.3 \times 10^{-4} T + 17.14 \times 10^{-3} M + 58.09 \times 10^{-6} T^2 - 10.12 \times 10^{-5} M^2 \quad (3.2)$$

where, k is thermal conductivity (W/m°C) and T is temperature (°C) and M is moisture content (%wb).

3.6 Specific Heat Capacity

For the specific heat capacity of zucchini, the equation obtained by Ali et al. (2002) was used;

$$C_p(T) = 4240 - 10 \times T + 7 \times 10^{-2} T^2 \quad (3.3)$$

where, C_p is specific heat capacity (J/kg°C) and T is temperature (°C).

3.7 Dielectric Properties

Barba et al. (2012) determined the dielectric constant and the dielectric loss factor of zucchini at 2.45 GHz and 22°C as 63.98 and 15.02, respectively. The dielectric properties were taken as constant. According to some studies (Funebo and Ohlsson, 1999; Sipahioglu and Barringer, 2003) the dielectric properties of cucumber, which resembles zucchini, changed with temperature and moisture content slightly. Almeida (2005) also assumed dielectric properties of potato during modeling of microwave-infrared combination heating as constant since they did not change with temperature, significantly.

For determination of microwave power by using Maxwell Equations dielectric properties of zucchini were considered in complex form as $63.98 - 15.02j$.

3.8 Heat Transfer Coefficient

Heat transfer coefficient for this study was selected as 30 W/m²K since Terres et al. (2014) showed that the heat transfer coefficient of zucchini was between 30-40

W/m²K during cooking. Moreover, according to Haldera and Datta (2012) and Hallstrom (1979) the heat transfer coefficients measured in baking ovens were in the range of 10-80 (W/m²K).

3.9 Modeling and Data Analysis

Study was divided into two parts in which microwave power was determined by using Maxwell Equations and Lambert Law. For both studies finite element modeling was applied and Comsol Multiphysics commercial software version 4.3 (Comsol Inc., Burlington, MA, USA) was used. Moreover, Root Mean Square Error (RMSE) and Standart Deviations were calculated by Microsoft Excel software package (Microsoft Corporation, USA) to carry out the statistical comparison of the experimental data with the model. Empirical models for parameters were obtained by using SigmaPlot 12.0 Programme (London, UK).

3.10 Modeling by Lambert Law

Since determination of microwave power by Lambert Law was based on the penetration depth of the food, entire oven was not modeled. The focus was just on the food.

Temperature and moisture content of zucchini were determined by using Lambert Law for microwave power determination with 2D axisymmetric drawing of the zucchini. When the solution was turned 360 degrees, cylindrical moisture and temperature distribution was obtained.

For Lambert assumption, the heat transfer interface and transport of diluted species interface were used. According to Comsol user guide, the heat transfer interface has the equations, boundary conditions, and sources for modeling conductive and convective heat transfer, and for solving the temperature. The dependent variable for the heat transfer interface is temperature T. For mass transfer of zucchini heated in microwave infrared combination oven, transport of diluted species interface was selected since it has the equations, boundary conditions, and rate expression terms for modeling mass transport of diluted species in solids and for solving for the

species concentrations. According to Comsol user guide, the settings for this physics interface can be chosen so as to simulate chemical species transport through diffusion (Fick's law) and convection. The dependent variable was the molar concentration, c .

The time dependent solver and the direct PARDISO solver were employed. With the direct solver the calculations took three minutes to reach to the final time of the process. For Lambert assumption since only food was modeled it was simple enough to solve 600 seconds of heating time. It took three minutes to solve for both T and c with Intel Core™ 2.40GHz, 16 GB computer. The microwave heating on off cycle was also considered according to the power level selected as 10, 30 and 50%.

3.10.1 Parameters Used for Modeling by Lambert Law

Parameters used to solve the equations are shown in Table 3.2.

Table 3.2 Parameters used for the simulation done by Lambert Law

Description	Expression
Air temperature of the oven	293.15[K]
Initial temperature of zucchini	293.15[K]
Density of zucchini	922[kg/m ³]
Initial moisture concentration of zucchini	95.85 [%]
Humidity of air (Chen et al., 1999)	2 [%]
Molar latent heat of vaporization	2.3×10 ⁶ [J/kg]
Heat transfer coefficient	30[W/(m ² K)]
Molecular weight of water	18[g/mol]
Radius of zucchini	16[mm]
Height of zucchini	30[mm]
Penetration depth	0.01[m]
On-off time for 10% microwave power	3 s on 37 s off
On-off time for 30% microwave power	14 s on 22 s off
On-off time for 50% microwave power	16 s on 22 s off

Zucchini was modeled as a 2D axisymmetric rectangular whose radius was 16 mm with length of 30 mm (Figure 3.4). When the rectangular segment was turned 360 degrees 3D cylinder was obtained.

On off time for different microwave powers (10, 30 and 50%) were added to the model as a piecewise analytic equation.

To fit the experimental data with the model, diffusion coefficient for evaporative loss (D_m), moisture diffusion coefficient in the food (D), mass transfer coefficient (k_c) and incident surface power (P_0) were determined in this study for different microwave (10, 30 and 50%) and infrared power (10, 40 and 70%) combinations.

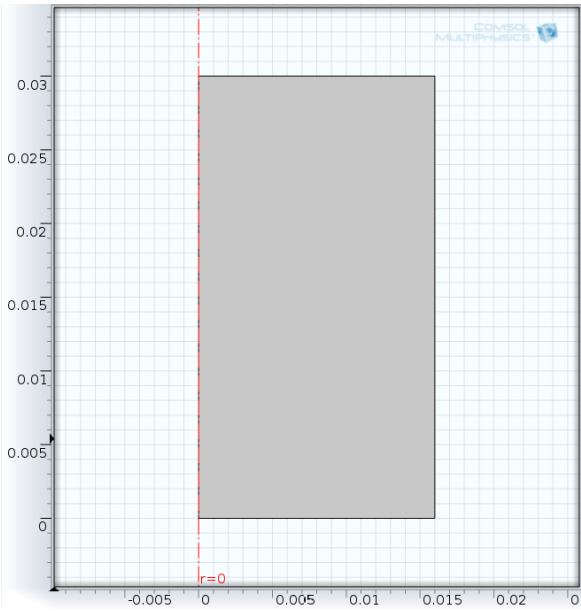


Figure 3.4 Sketch of 2D axisymmetric rectangular model of zucchini

3.10.2 Mesh Properties for Modeling by Lambert Law

As can be seen from Figure 3.5, only zucchini was meshed. Minimum element quality, average element quality, the number of triangular elements, edge elements, vertex elements, maximum and minimum element size, resolution of curvature and maximum element growth rate were tabulated at Table 3.3 and 3.4. Mesh convergence test was done to define optimum mesh size.

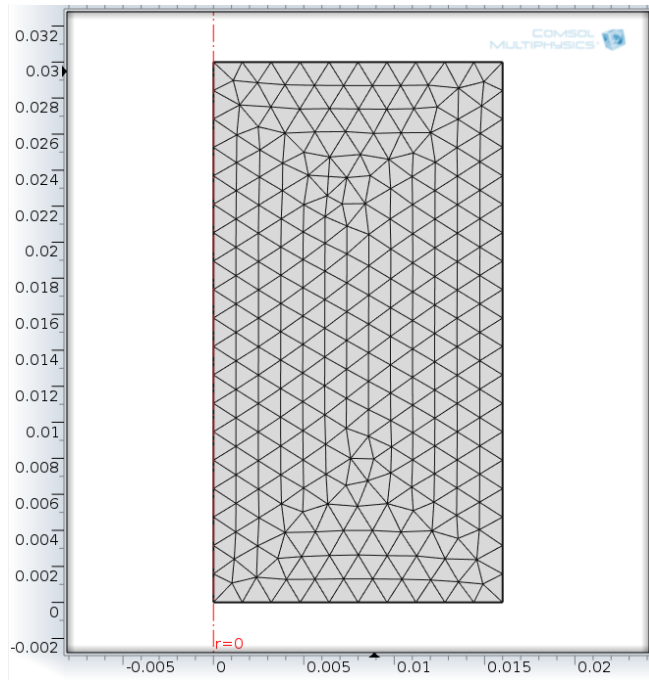


Figure 3.5 Meshed 2D axisymmetric rectangular model of zucchini

Table 3.3 Mesh properties

Property	Value
Minimum element quality	0.7679
Average element quality	0.9801
Triangular elements	494
Edge elements	58
Vertex elements	4

Table 3.4 Mesh size

Name	Value
Maximum element size	0.00159
Minimum element size	$9 \cdot 10^6$
Resolution of curvature	0.30000
Maximum element growth rate	1.30000
Predefined size	Fine

3.10.3 Infrared Boundary Condition for Modeling by Lambert Law

The infrared heating of the surface of the food was considered in the model as surface to ambient radiation boundary condition using the Equation (2.37). Surface temperature of the halogen lamp was assumed to be 750K, 800K and 850K for 10%, 40% and 70% infrared powers, respectively. Surface emissivity of zucchini was assumed to be 0.9.

3.10.4 Heat Flux Boundary Condition for Modeling by Lambert Law

Convective heat loss and evaporative heat losses were modeled using heat flux boundary condition at the surface of the food in both radial and axial directions separately, using the Equation (2.8).

3.10.5 Mass transfer model setup for Modeling by Maxwell Equations

Program's transport of diluted species module was used in order to solve the mass transfer equation which was shown in Equation (2.1). Initial condition (Equation 2.4), the symmetry boundary condition (Equation 2.5), convective mass transfer loss (Equation 2.7) were added into the transport of diluted species module.

3.11 Modeling by Maxwell Equations

In order to determine the electric field distribution from the rectangular waveguide, Maxwell Equations were solved for the entire oven. Oven was cut in to two and symmetry condition was considered in order to simplify and decrease the time of the solution. Oven was assumed to have a rectangular waveguide and drawn as a rectangular box together and zucchini was placed at the center on the porcelain plate.

For electromagnetic heating, microwave heating interface of radio frequency module was selected. According to Comsol user guide, the microwave heating interface combines the features of an electromagnetic waves interface with those of the heat transfer interface and shares most of its settings with electromagnetic waves, frequency domain interface, the heat transfer interface and the joule heating interface. Dependent variables of microwave heating interface are electric field (E),

surface radiosity (J) and temperature (T). The electromagnetic losses from the electromagnetic waves were used as a heat source.

For mass transfer of zucchini heated in microwave infrared combination oven, transport of diluted species interface was selected since it has the equations, boundary conditions, and rate expression terms for modeling mass transport of diluted species in solids, solving for the species concentrations. According to Comsol user guide, the settings for this physics interface can be chosen so as to simulate chemical species transport through diffusion (Fick's law), convection. The dependent variable of transport of diluted species interface is the molar concentration, c .

In microwave heating and transport of diluted species interfaces appropriate initial and boundary conditions and rate expression terms were added.

Maxwell's equations for electromagnetics were solved using time dependent solver, the biconjugate gradient stabilized method (BiCGStab) and a developed minimum residual solver with geometric multi grid preconditioner (GMRES) iterative solvers. The transport of diluted species used PARDISO direct solver. Solving equations with boundary conditions to determine electric field, temperature and moisture content distributions took 15 hours to reach the final time of the process with Intel Core™ 2.40GHz, 16 GB computer. Strict time stepping was selected to catch the on off cycling conditions properly. For simplicity, in Maxwell modeling 100 seconds of heating time was considered since it took 144 hours for 600 seconds solution. The microwave and infrared heating on off cycle was considered according to the power level selected as 10, 30 and 50%.

3.11.1 Parameters Used for Modeling by Maxwell Equations

Parameters used to solve the equations are shown in Table 3.5.

Table 3.5 Parameters used for the simulation done by Maxwell Equations

Description	Expression
Width of the oven	470[mm]
Depth of the oven	356[mm]
Height of the oven	215[mm]
Width of the waveguide	$(86.36/2)$ [mm]
Depth of the waveguide	70[mm]
Height of the waveguide	43.13[mm]
Radius of the glass plate	150[mm]
Height of the glass plate	20[mm]
Base of the glass plate	15[mm]
Radius of the zucchini	16[mm]
Height of the zucchini	30[mm]
Initial temperature of the zucchini	20[°C]
Molar weight of water	18[g/mol]
Initial concentration of the zucchini	95.85 [%]
Density of the zucchini	922[kg/m ³]
The molar latent heat of vaporization	2.3×10^6 [J/kg]
Heat transfer coefficient	30[W/(m ² K)]
Air temperature in the oven	20[°C]
Humidity of air (Chen et al., 1999)	2 [%]
On-off time for 10% microwave power Port input power when 10% microwave power selected ($618 \times 0.10 = 61.8$)	7 s on 38 s off 61.8 [W]

The oven was drawn as a rectangular box together with rectangular waveguide and at the center zucchini was placed on the porcelain plate as shown in Figure 3.6.

Both microwave and infrared heating system in the oven works with cycles on and off. Since 100 seconds of heating was modeled both microwave and infrared cycling was considered. On off time was added to the model as a piecewise analytic equation.

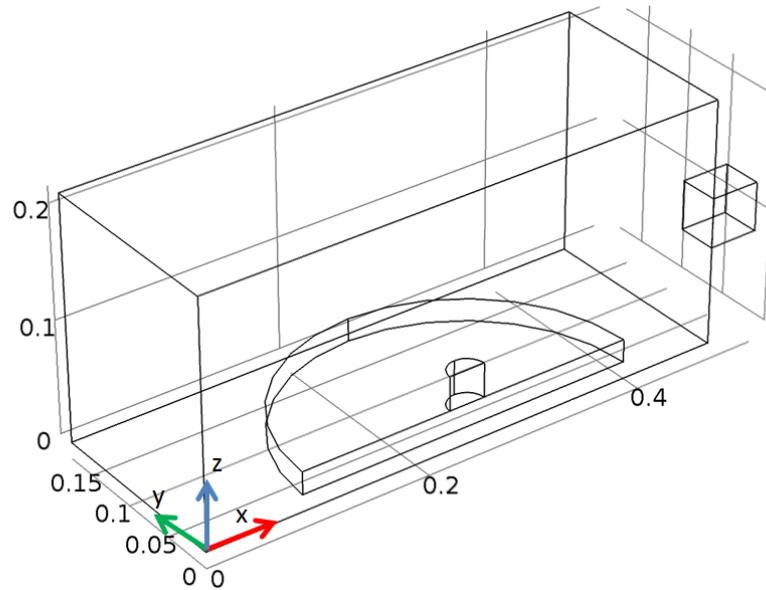


Figure 3.6 Sketch used for modeling of the entire oven together with rectangular waveguide and zucchini

3.11.2 Explicit Selections for Modeling by Maxwell Equations

Cylindrical object at the center of the oven was named as zucchini (Figure 3.7).

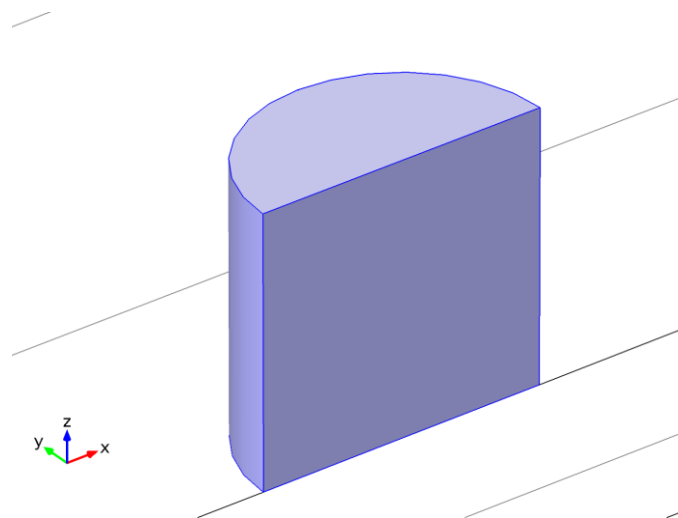


Figure 3.7 Sketch used for modeling of the zucchini

Plate inside the oven was named as porcelain plate. The material inside the oven and rectangular waveguide was chosen as air, and they are selected as no heat transfer

medium. Right side of the rectangular waveguide was selected as port boundary. Oven and rectangular waveguide's walls was made up of stainless steel thus they are named as metal boundaries.

3.11.3 Material Properties for Modeling by Maxwell Equations

Properties of air, porcelain and structural steel were taken from the library of the program and represented in Table 3.6.

Table 3.6 Properties of air, silicon carbide (porcelain) and structural steel

	Air	Silicon carbide (porcelain)	Structural steel
Relative permeability	1	1	1
Relative permittivity	1	10	1
Electrical conductivity [S/m]	0	10 ³	4.02 × 10 ⁶

3.11.4 Mesh Properties for Modeling by Maxwell Equations

Entire oven was meshed and especially zucchini's mesh was selected to be finer than the rest of the system as can be seen from Figure 3.8. Minimum element quality, average element quality, the number of tetrahedral elements, triangular elements, edge elements and vertex elements together with mesh size such as: maximum and minimum element size, resolution of curvature and maximum element growth rate were tabulated at Table 3.7 and 3.8. Mesh convergence test was done to define optimum mesh size.

Table 3.7 Mesh properties

Property	Value
Minimum element quality	0.1317
Average element quality	0.7022
Tetrahedral elements	4429
Triangular elements	1200
Edge elements	186
Vertex elements	28

Table 3.8 Mesh size

Name	Value
Maximum element size	0.05130
Minimum element size	0.00924
Resolution of curvature	0.60000
Resolution of narrow regions	0.50000
Maximum element growth rate	1.50000

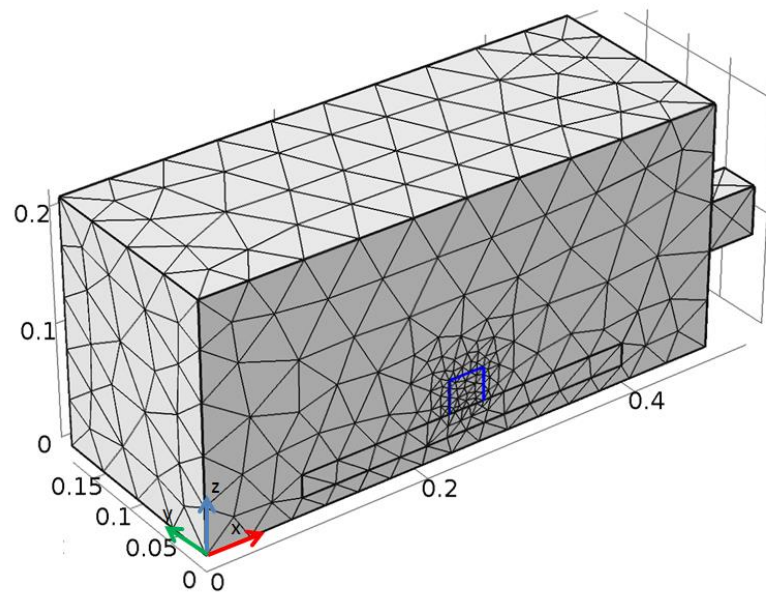


Figure 3.8 Sketch of meshed oven

3.11.5 Microwave Heating Model Setup for Modeling by Maxwell Equations

Microwaves were considered to dissipate through the oven from the right end of the rectangular waveguide (Figure 3.9) with TE₁₀ mode propagation. Initially, the electric field in the oven in x,y,z direction was zero as shown in Equation (2.19). Excitation of electric field in the z direction was entered the program by using Equation (2.20). Propagation constant was calculated from Equation (2.17).

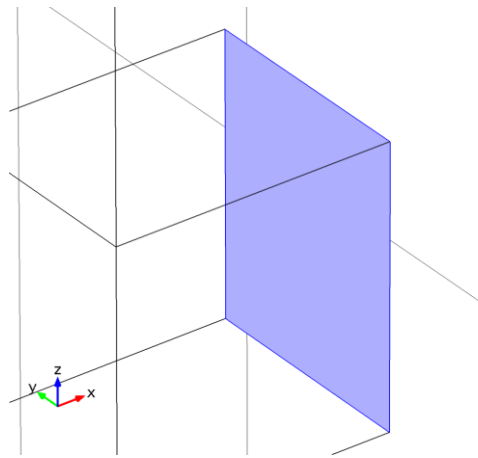


Figure 3.9 Sketch of port boundary

Comsol Multiphysics software gave rise to select the metal boundaries, walls of the oven and the rectangular waveguide shown by Figure 3.10 as the impedance boundary condition. According to software manual, impedance boundary condition was used where the electric field was known to penetrate only a short distance outside the boundary and the penetration was approximated in order to avoid addition of another domain to the model. Thus, this boundary was used on exterior boundaries representing the surface of a lossy domain even it was not included in the model.

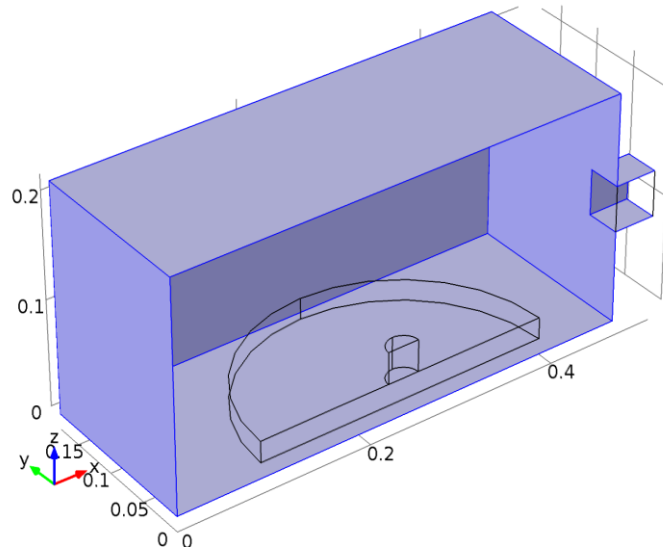


Figure 3.10 Sketch of metal boundaries

Figure 3.11 shows the symmetry boundary which was assumed to be perfect magnetic conductor.

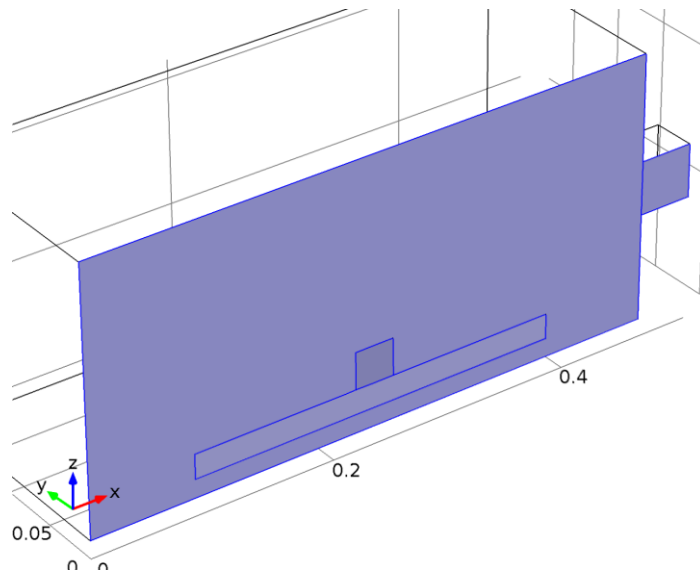


Figure 3.11 Sketch of symmetry boundary

3.11.6 Infrared Boundary Condition for Modeling by Maxwell Equations

The infrared heating of the surface of the food was considered in the model as surface to ambient radiation boundary condition using the Equation (2.37). Surface temperature of the halogen lamp was assumed to be 750K, 800K and 850K for 10%, 40% and 70% infrared powers, respectively. Surface emissivity of zucchini was assumed to be 0.9.

3.11.7 Heat Flux Boundary Condition for Modeling by Maxwell Equations

Convective heat loss and evaporative heat losses were modeled using heat flux boundary condition at the surface of the food in both radial and axial directions separately, using the Equation (2.8).

3.11.8 Mass Transfer Model Setup for Modeling by Maxwell Equations

Program's transport of diluted species module was used in order to solve the mass transfer equation which was shown in Equation (2.1). Initial condition (Equation 2.4), the symmetry boundary condition (Equation 2.5), convective mass transfer loss (Equation 2.7) were added into the transport of diluted species module.

CHAPTER 4

RESULTS AND DISCUSSION

In the first part of the study, temperature data at different positions ($r=0.0, 6.1$ and 10.5 mm) of the zucchini sample and moisture content of zucchini heated in microwave infrared combination oven at different microwave power (10, 30 and 50%) and infrared powers (10, 40 and 70%) for 600 s were compared with the model obtained based on Lambert Law. Temperature data of the model were obtained by taking the line average of the temperature results along a line which extends from $z=11$ to $z=18$ mm, $z=11$ to $z=18$ mm and $z=25$ to $z=30$ for the temperatures at positions $r=10.5, 0.0$ and 6.1 mm, respectively.

In the second part of the study, empirical models for variation of moisture diffusion coefficient (D), mass transfer coefficient (k_c) and incident surface power (P_0) as a function of microwave and infrared powers were developed.

In the third part of the study, models obtained based on Maxwell Equations were validated with temperature data at different positions ($r=0.0, 6.1$ and 10.5 mm) of the zucchini sample and moisture content of zucchini heated in microwave infrared combination oven at microwave power (10%) and different infrared powers (10%, 40% and 70%) for 100 s.

In the fourth part of the study, the effects of microwave and infrared power on temperature distribution and moisture content of zucchini were analyzed by showing experimental and model results obtained based on Lambert Law. Furthermore, the variation of temperature and moisture content with respect to position in the zucchini specimen was analyzed.

In the last part of the study, models obtained by Maxwell Equations and Lambert Law were compared.

4.1 Experimental and Model Results Based on Lambert Law

Cylindrical zucchini samples with a height of 30 ± 1 mm and a diameter of 32 ± 1 mm were heated in microwave infrared combination oven by adjusting different microwave (10%, 30%, 50%) and infrared (10%, 40%, 70%) powers for 600 seconds. Temperature data at different points of the zucchini ($r=0.0, 6.1$ and 10.5 mm) and moisture content data were used to validate mathematical models.

In order to solve heat (Equation 2.2) and mass (Equation 2.1) transfer equations by finite element method, initial conditions (Equations 2.3 and 2.4), symmetry boundary condition (Equations 2.5 and 2.6) and convective boundary condition (Equations 2.7 and 2.8) were used with parameters listed at Table 3.2. Power term at Equation (2.2) was predicted by the exact form of Lambert Law derived by making shell balance (Equation 2.36).

Different parameters (incident surface power, moisture diffusion coefficient in the food, the diffusion coefficient for evaporative loss and mass transfer coefficient) were determined in this study for different microwave and infrared power combinations to fit model to the experimental data represented in Table 4.1.

Figure 4.1-4.9 show the temperature distribution at three different locations of the zucchini ($r=10.5, 0.0$ and 6.1 mm) and moisture content with the model obtained by Lambert Law for different microwave and infrared combination.

Heat and mass transfer model were coupled by the evaporative heat loss term at the surface shown by $D_m \lambda \nabla c$ in Equation (2.8). It was added to the model to reflect that the change in the concentration had an impact on the temperature decrease at the surface.

At first, diffusion coefficient in the food (D) and diffusion coefficient for evaporative loss (D_m) were assumed to be the same in this study. Tavakolipour et al. (2014), found the effective moisture diffusion of zucchini in a fan dryer as 1.85×10^{-8} - 11.4×10^{-8} m^2/s . These results were used as an initial assumption. However, no fit was observed between measured data and the model. Thus, it was thought that D should be lower than D_m because of the porous structure of the food. Differences in the diffusivities were also observed by Malafronte et. al. (2012) and Chen et. al. (1999). Moreover, it can be seen from Table 4.1 that as microwave power increased, the difference in the diffusivity values decreased. Internal heating of microwaves results in generation of pressure gradient of vapor from the interior to the surface of the product. As microwave power increases the interior pressure increases so that the porosity of the food can no longer be a barrier to flow. Thus, under high microwave power less differences in diffusivity values were observed.

Both microwave and infrared heating system in the oven works with cycles on and off. Since microwave heating dominates the overall mechanism only on off cycle of microwave heating was considered. On and off time changed with different microwave powers. Figure 4.1-4.9 showed the stair like, pulsed temperature profile which resulted from on off cycles.

As can be seen from Table 4.2 that temperature models were in good agreement with the measured data with root mean square error (RMSE) ranging from 2.44 to 9.37 with an average of 5.66. RMSE for moisture content ranged from 0.16 to 5.68 with an average of 2.52.

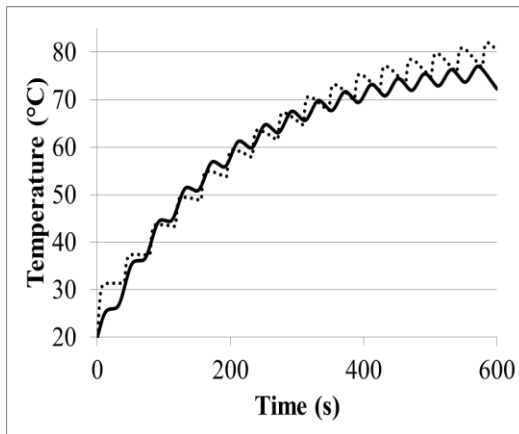
Chen et. al. (2014) modeled the heat and mass transport of mashed potato during microwave heating at 6 locations of potato. Temperature data were in good agreement with predicted results, with the root mean square error ranging from 1.6 to 11.7 °C. Pitchai (2015) developed a finite element model for microwave heat transfer of frozen multi-component foods. Model was validated with experimental data. The simulated temperature profile was found to be in good agreement with experimental temperature profile with RMSE values ranging from 6.6 °C to 20.0 °C. Thus, RMSE values of this study were in accepted range.

Table 4.1 Parameter values obtained for models based on Lambert Law for different microwave and infrared power operating conditions

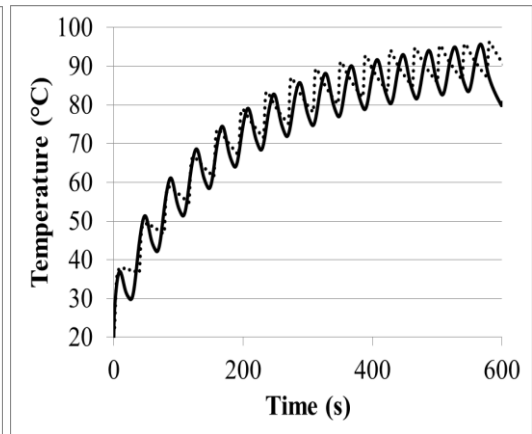
MWP (%)	IRP (%)	P_0 (W)	D (m^2/s)	$D_m(T)$ (m^2/s)	k_c (m/s)
10	10	160000	10^{-12}	$(20 + 2T^{0.008} + 10^{-6}T^2)10^{-9}$	2.2×10^{-7}
10	40	160000	10^{-12}	$(20 + 2T^{0.008} + 10^{-6}T^2)10^{-9}$	3×10^{-7}
10	70	160000	10^{-12}	$(20 + 2T^{0.008} + 10^{-6}T^2)10^{-9}$	6×10^{-7}
30	10	300000	5×10^{-9}	$(20 + 2T^{0.008} + 10^{-5}T^2)10^{-9}$	5×10^{-6}
30	40	300000	5×10^{-9}	$(20 + 2T^{0.008} + 10^{-5}T^2)10^{-9}$	8×10^{-5}
30	70	300000	7×10^{-9}	$(20 + 2T^{0.008} + 10^{-5}T^2)10^{-9}$	8×10^{-5}
50	10	300000	1×10^{-8}	$(20 + 200T^{0.008} + 10^{-5}T^2) \times 9 \times 10^{-8}$	8×10^{-5}
50	40	300000	1.5×10^{-8}	$(20 + 200T^{0.008} + 10^{-5}T^2) \times 9 \times 10^{-8}$	2×10^{-4}
50	70	300000	1.5×10^{-8}	$(20 + 200T^{0.008} + 10^{-5}T^2) \times 10^{-8}$	2×10^{-4}

Table 4.2 Root mean square errors (RMSE) calculated by experimental data and models obtained based on Lambert Law for temperature at different positions of zucchini and moisture content.

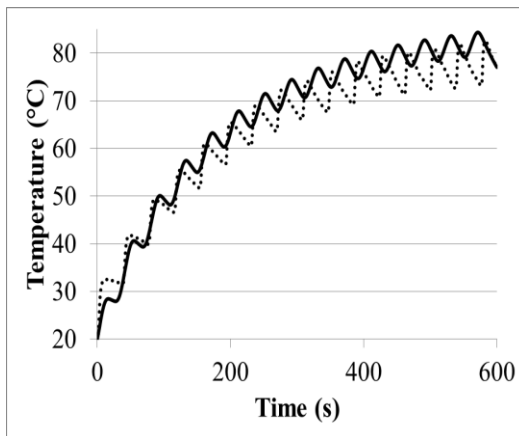
MWP (%)	IRP (%)	Temperature			Moisture Content
		r=10.5	r=0.0	r=6.1	
10	10	3.27	5.39	4.48	0.16
10	40	2.44	5.07	4.61	0.35
10	70	3.21	6.01	5.34	0.35
30	10	5.93	7.76	7.39	3.08
30	40	5.96	4.62	7.19	3.61
30	70	5.55	3.65	5.52	3.93
50	10	5.69	6.00	8.01	2.76
50	40	6.41	5.89	5.91	2.74
50	70	5.14	6.97	9.37	5.68



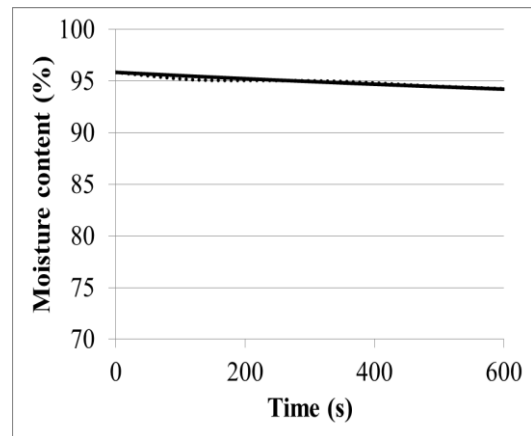
(a)



(b)

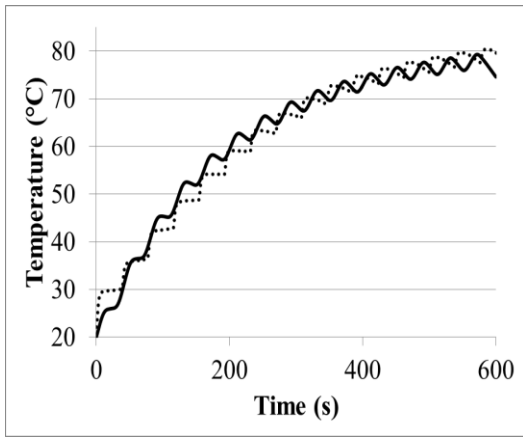


(c)

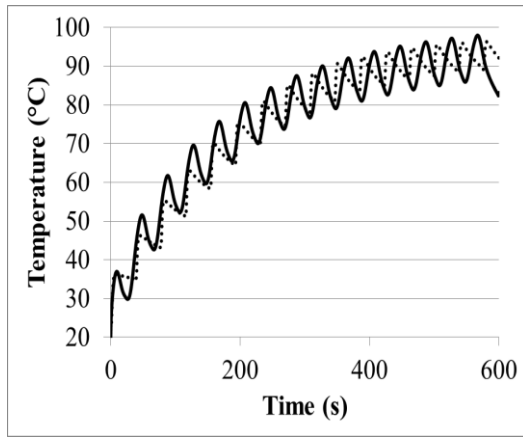


(d)

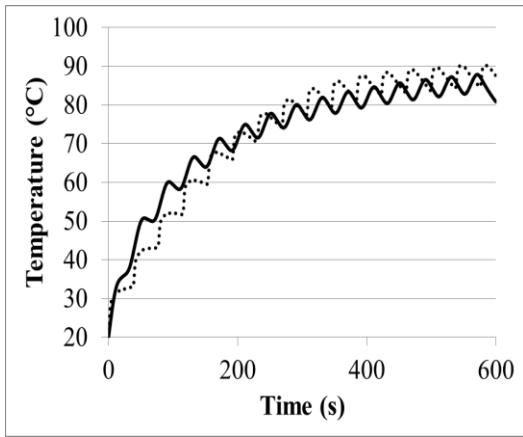
Figure 4.1 Lambert model (line) and experimental (dotted line) results of temperature at (a) $r=10.5$ mm, (b) $r=0.0$ and (c) $r=6.1$ mm and (d) moisture content of zucchini heated by 10% microwave and 10% upper infrared power.



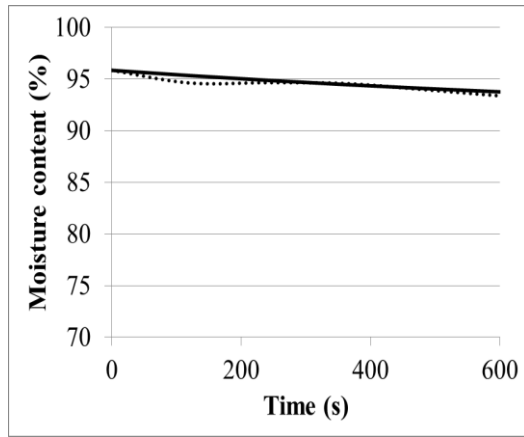
(a)



(b)

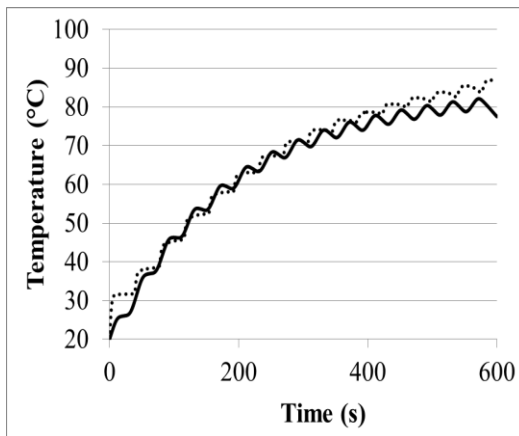


(c)

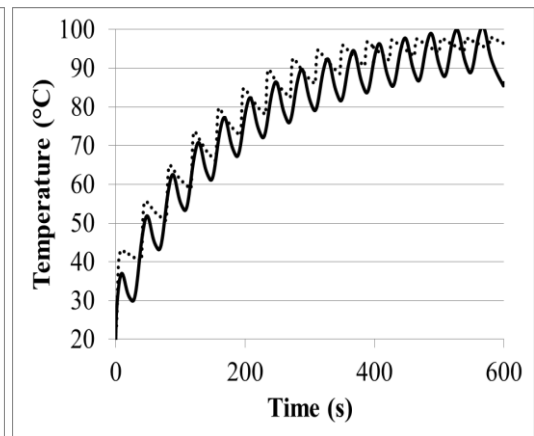


(d)

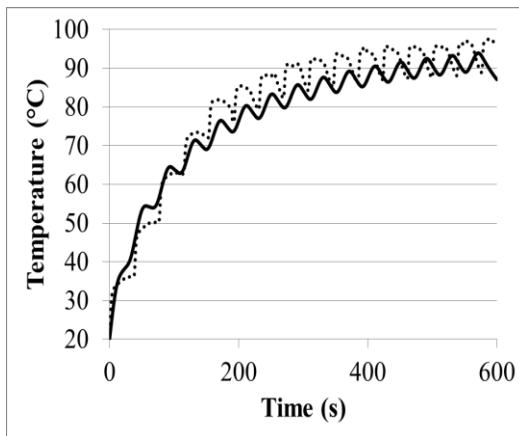
Figure 4.2 Lambert model (line) and experimental (dotted line) results of temperature at (a) $r=10.5$ mm, (b) $r=0.0$ and (c) $r=6.1$ mm and (d) moisture content of zucchini heated by 10% microwave and 40% upper infrared power.



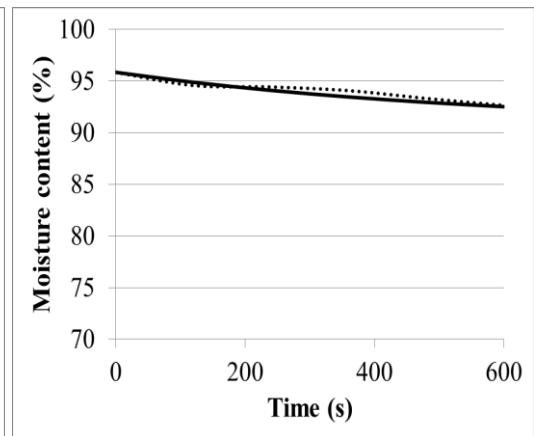
(a)



(b)

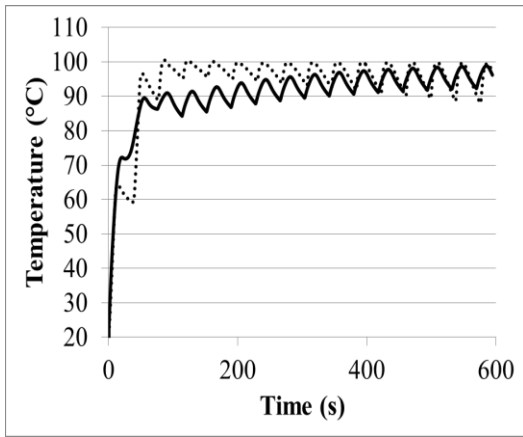


(c)

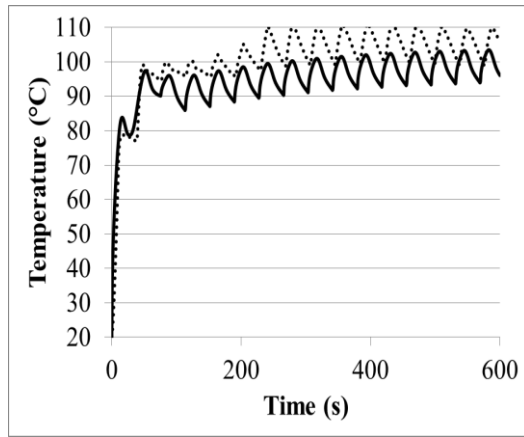


(d)

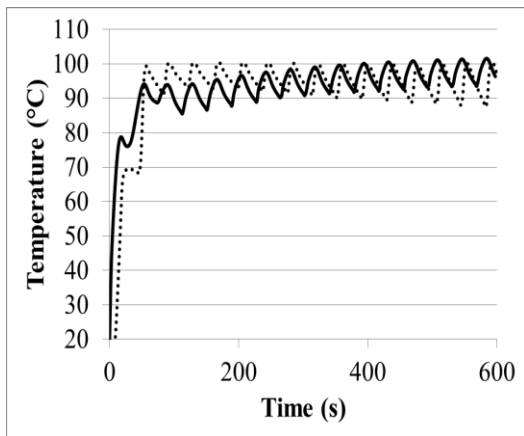
Figure 4.3 Lambert model (line) and experimental (dotted line) results of temperature at (a) $r=10.5$ mm, (b) $r=0.0$ and (c) $r=6.1$ mm and (d) moisture content of zucchini heated by 10% microwave and 70% upper infrared power.



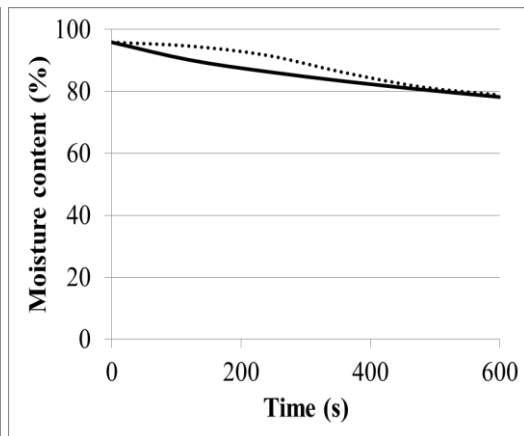
(a)



(b)

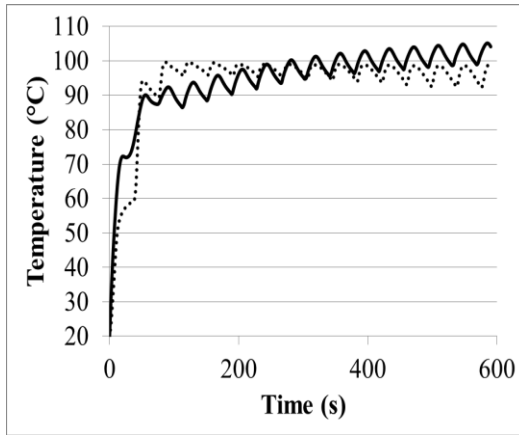


(c)

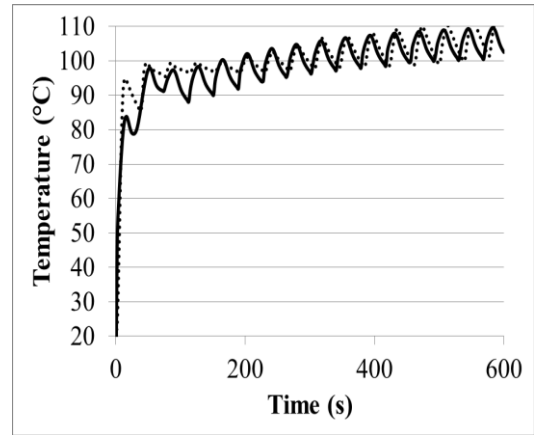


(d)

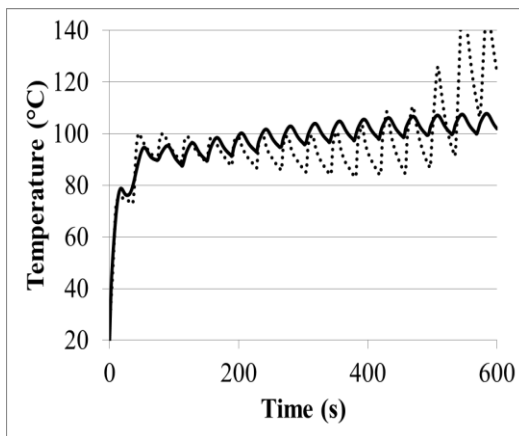
Figure 4.4 Lambert model (line) and experimental (dotted line) results of temperature at (a) $r=10.5$ mm, (b) $r=0.0$ and (c) $r=6.1$ mm and (d) moisture content of zucchini heated by 30% microwave and 10% upper infrared power.



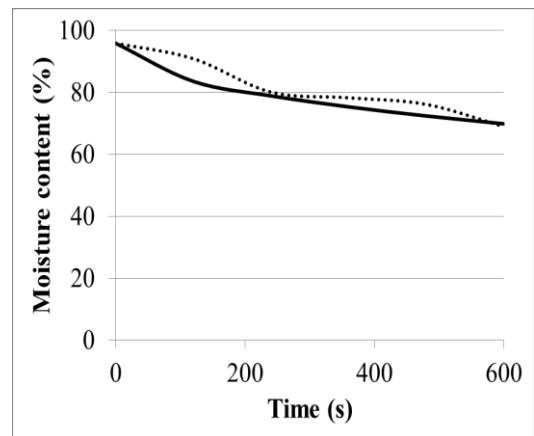
(a)



(b)

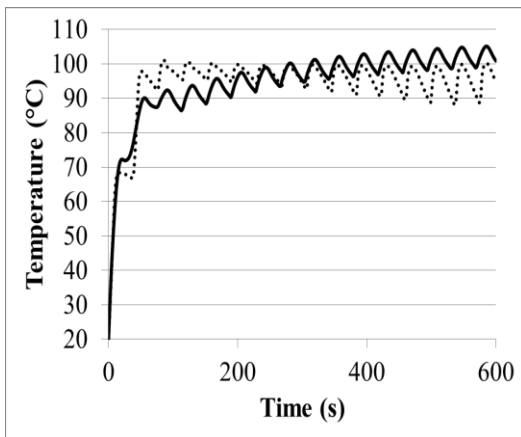


(c)

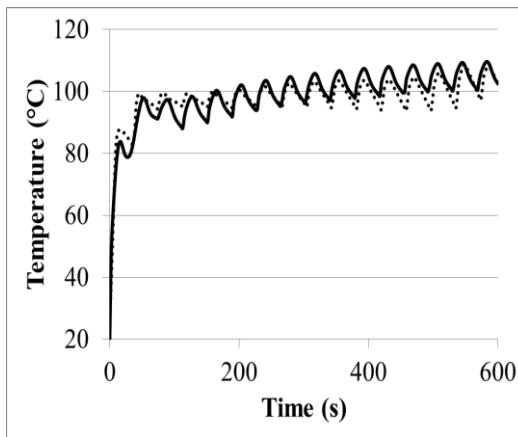


(d)

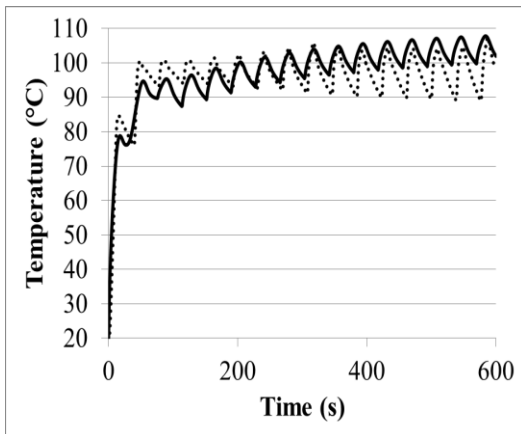
Figure 4.5 Lambert model (line) and experimental (dotted line) results of temperature at (a) $r=10.5$ mm, (b) $r=0.0$ and (c) $r=6.1$ mm and (d) moisture content of zucchini heated by 30% microwave and 40% upper infrared power.



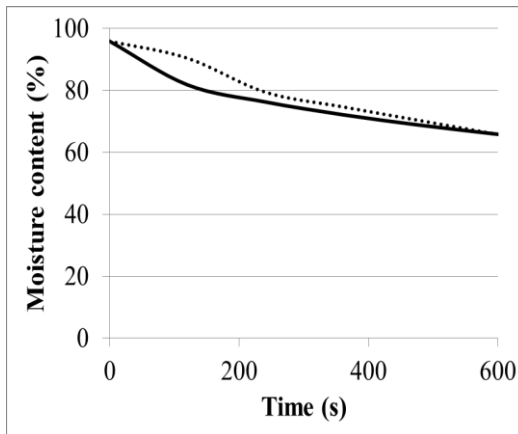
(a)



(b)

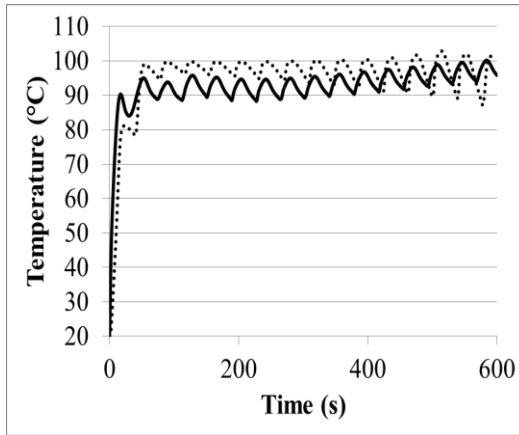


(c)

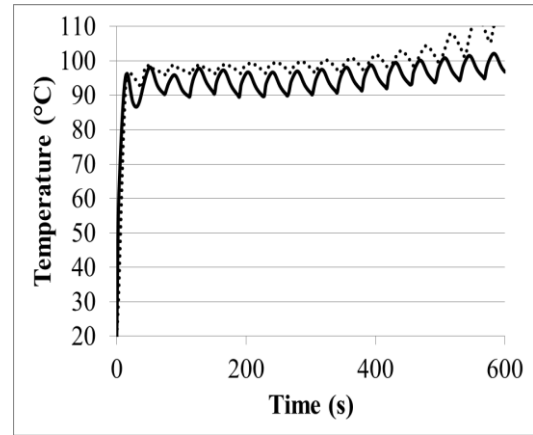


(d)

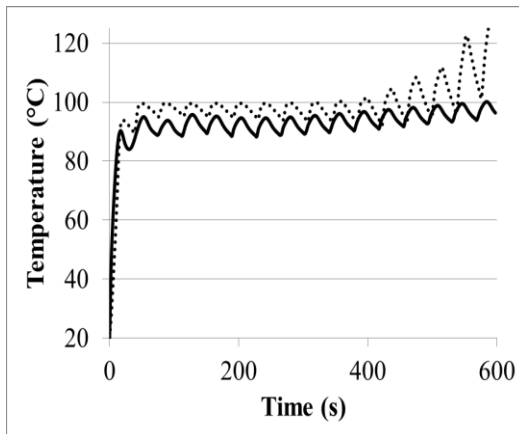
Figure 4.6 Lambert model (line) and experimental (dotted line) results of temperature at (a) $r=10.5$ mm, (b) $r=0.0$ and (c) $r=6.1$ mm and (d) moisture content of zucchini heated by 30% microwave and 70% upper infrared power.



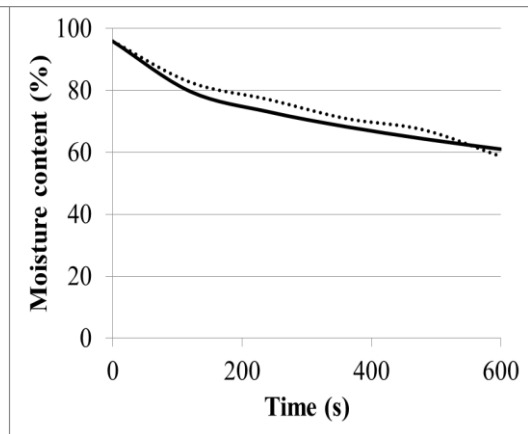
(a)



(b)

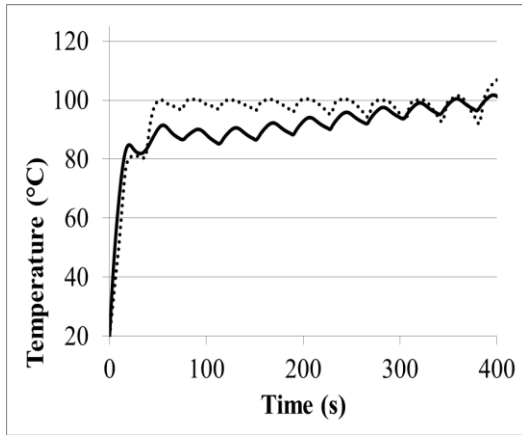


(c)

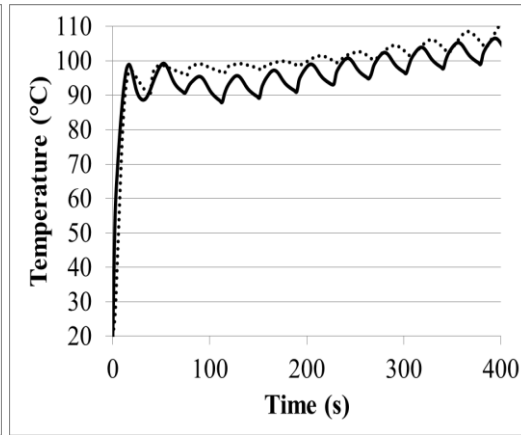


(d)

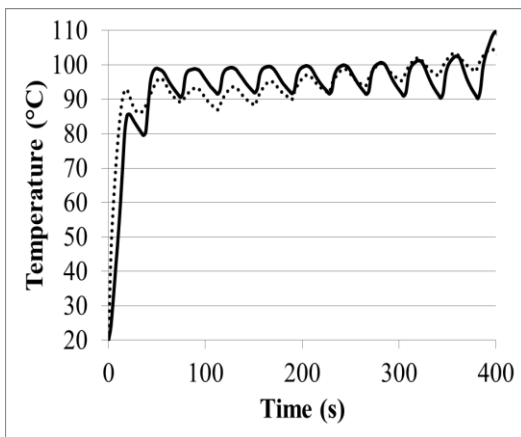
Figure 4.7 Lambert model (line) and experimental (dotted line) results of temperature at (a) $r=10.5$ mm, (b) $r=0.0$ and (c) $r=6.1$ mm and (d) moisture content of zucchini heated by 50% microwave and 10% upper infrared power.



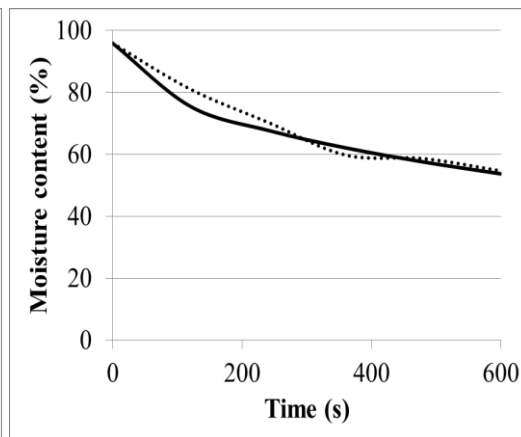
(a)



(b)



(c)



(d)

Figure 4.8 Lambert model (line) and experimental (dotted line) results of temperature at (a) $r=10.5$ mm, (b) $r=0.0$ and (c) $r=6.1$ mm and (d) moisture content of zucchini heated by 50% microwave and 40% upper infrared power.

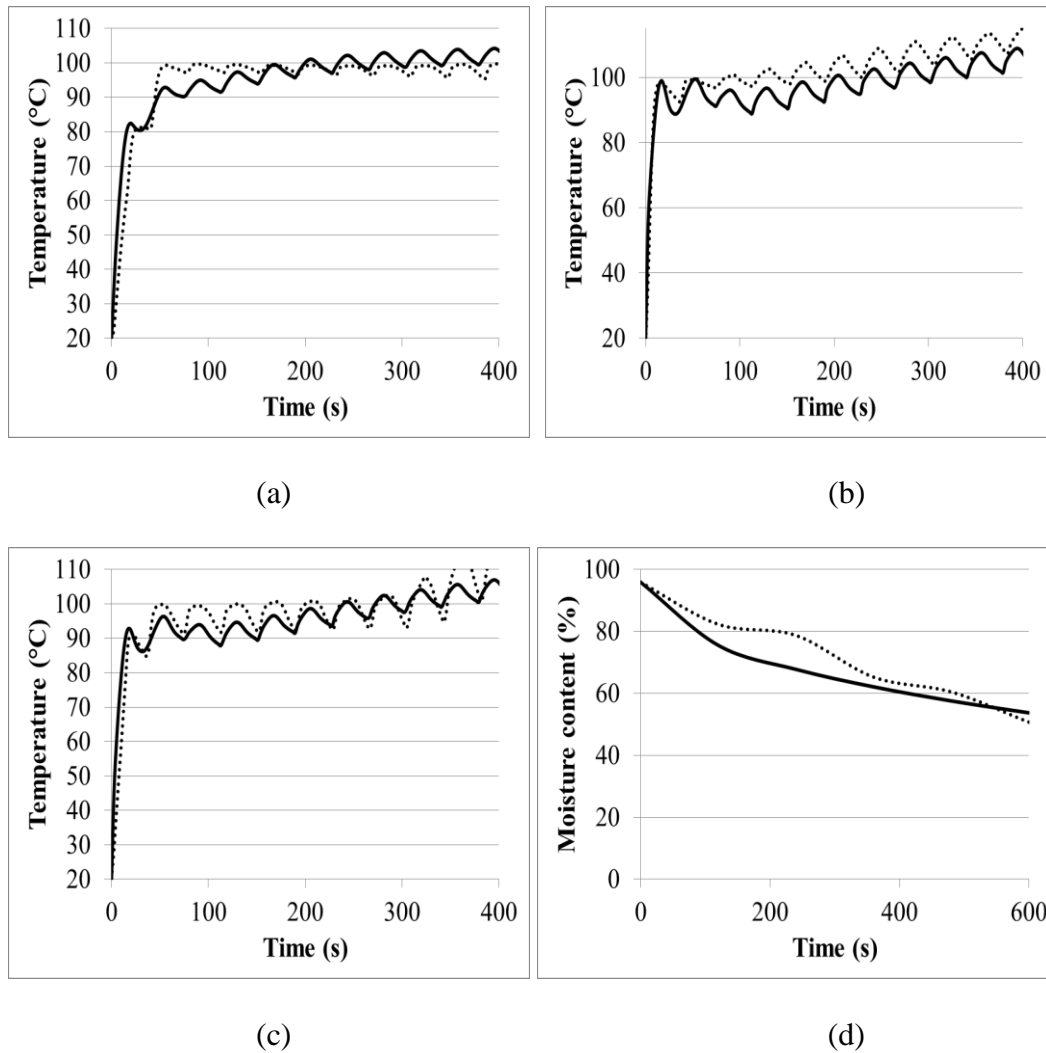


Figure 4.9 Lambert model (line) and experimental (dotted line) results of temperature at (a) $r=6.1$ mm, (b) $r=0.0$ and (c) $r=10.5$ mm and (d) moisture content of zucchini heated by 50% microwave and 70% upper infrared power.

4.2 Empirical Modeling of Parameters Obtained for Models Based on Lambert Law

In this study, to fit the experimental data with the model obtained by Lambert Law, incident surface power, moisture diffusion coefficient in the food and mass transfer coefficient were changed with respect to microwave and infrared powers. To better understand the Lambert models, it was necessary to study the effects of microwave and infrared powers on these parameters. Empirical models were obtained as a

function of microwave (%MWP) and infrared power (%IRP) by using SigmaPlot 12.0 Programme.

Since incident surface power and moisture diffusion coefficient were directly related to microwave power, they were modelled as a function of microwave power with high coefficient of determination (R^2) values 1.00 and 0.93, respectively. However, it was observed in this study that as both microwave and infrared power increased mass transfer coefficient increased. Mass transfer coefficient was modelled as a function of microwave (MWP) and infrared power (IRP) with satisfactory coefficient of determination value, 0.99.

Table 4.3 Empirical models for parameters

Parameter	Equation	R^2
P_0 (W)	$= 37500 + 14000 * MWP - 175 * (MWP)^2$	1.00
D (m^2/s)	$= -2.989 \times 10^{-9} + 3.2239 \times 10^{-10} \times (MWP) - 2.9441 \times 10^{-12} \times (MWP)^2 + 6.0503 \times 10^{-14} \times (MWP)^3$	0.93
k_c (m/s)	$= 0.0003 \times e^{(-0.5(((MWP-44.7217)/9.8363)^2 + ((IRP-55.0001)/29.5081)^2))}$	0.99

Where microwave and infrared powers' unit was percent (%).

By the help of these empirical models, it would be possible to operate the oven for different microwave and infrared power combinations and to use the models for temperature and moisture derived from Lambert Law.

4.3 Experimental and Model Results Based on Maxwell Equations

Cylindrical zucchini samples with a height of 30 ± 1 mm and a diameter of 32 ± 1 mm were heated in microwave infrared combination oven by adjusting microwave (10%) and infrared (10%, 40%, 70%) powers for 100 s. Measured temperature at different points of the zucchini ($r=0.0, 6.1$ and 10.5 mm) and interpolated moisture content data of 600 s were used to validate mathematical models.

In order to solve heat transfer (Equation 2.2), mass transfer (Equation 2.1), and electromagnetic (2.14) equations by finite element method, initial conditions (Equations 2.3, 2.4 and 2.19), symmetry boundary condition (Equations 2.5, 2.6, 2.15 and 2.16) and convective boundary condition (Equations 2.7 and 2.8) were used with parameters listed at Table 3.5. Power term (Q_{gen}) at Equation (2.2) was estimated by using Equation (2.9) where electric field distribution was calculated by Maxwell Equations (2.10, 2.11, 2.12 and 2.13).

In this study, in order to fit the model to experimental data, D_m (the diffusion coefficient for evaporative loss), D (moisture diffusion coefficient) and k_c (mass transfer coefficient) were determined for different microwave infrared power combinations and represented at Table 4.4.

Figure 4.10-4.12 show the experimental temperatures at three different locations of the zucchini ($r=10.5, 0.0$ and 6.1 mm) and moisture content with the model obtained by Maxwell Equations for different microwave and infrared combination.

Electromagnetics and heat transfer were coupled by the calculation of microwave power term. Whereas heat and mass transfer model were coupled by the evaporative heat loss term at the surface shown by $D_m \lambda \nabla c$ in Equation (2.8). It was added to the model to reflect that the change in the concentration had an impact on the temperature decrease at the surface.

As was discussed in section 4.1, diffusion coefficient in the food (D) and diffusion coefficient for evaporative loss (D_m) were first assumed to be the same. Since no fit was observed, it was thought that D should be lower than D_m because of the porous structure of the food. Similar difference in the diffusivity values were observed by Malafrente et. al. (2012) and Chen et. al. (1999).

Both microwave and infrared heating system in the oven works with cycles on and off. Since 100 seconds of heating was modeled, both microwave and infrared cycling was considered for more precise modeling. Thus, on off cycle time was assumed to

be slightly different than models obtained by Lambert Law. Figure 4.10-4.12 showed the stair like, pulsed temperature profile which resulted from on off cycles.

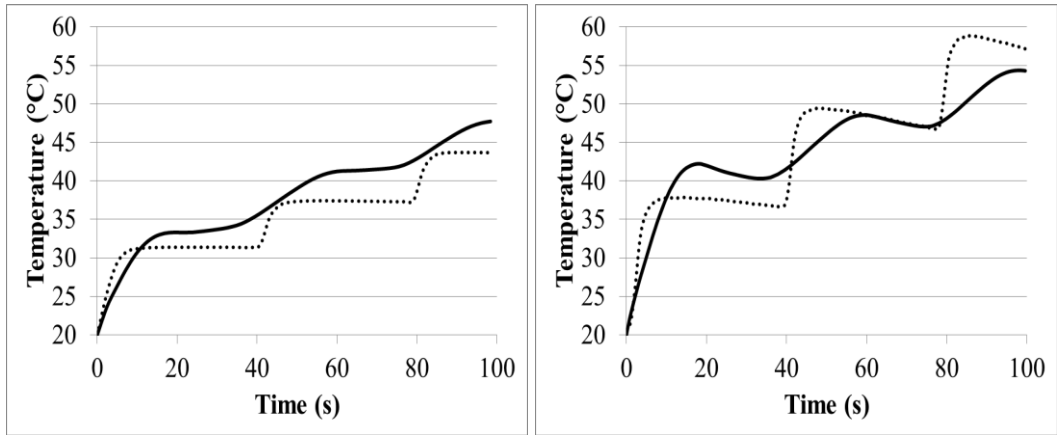
As can be seen from Table 4.5 that temperature models were in good agreement with the measured data with root mean square error (RMSE) ranging from 1.97 to 5.77 with an average of 4.15. RMSE for moisture content ranged from 0.19 to 0.49 with an average of 0.39.

Table 4.4 Parameter values obtained for models based on Maxwell Equations for different microwave and infrared power operating conditions

MWP (%)	IRP (%)	D (m ² /s)	D _m (T) (m ² /s)	k _c (m/s)
10	10	10 ⁻¹²	(20 + 2T ^{0.008} + 10 ⁻⁶ T ²)10 ⁻⁹	2.2 × 10 ⁻⁷
10	40	10 ⁻¹²	(20 + 2T ^{0.008} + 10 ⁻⁶ T ²)10 ⁻⁹	2.2 × 10 ⁻⁷
10	70	10 ⁻¹²	(20 + 2T ^{0.008} + 10 ⁻⁶ T ²)10 ⁻⁹	2.2 × 10 ⁻⁷

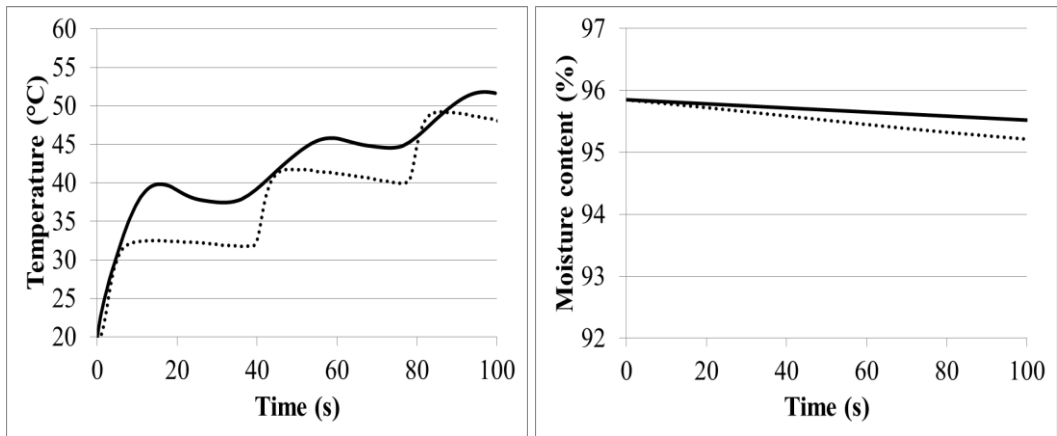
Table 4.5 Root mean square errors (RMSE) calculated by experimental data and models obtained based on Maxwell Equations for temperature at different positions of zucchini and moisture content.

MWP (%)	IRP (%)	Temperature			Moisture Content
		r=10.5	r=0.0	r=6.1	
10	10	2.96	3.95	4.38	0.19
10	40	1.97	4.59	5.77	0.48
10	70	2.85	5.40	5.51	0.49



(a)

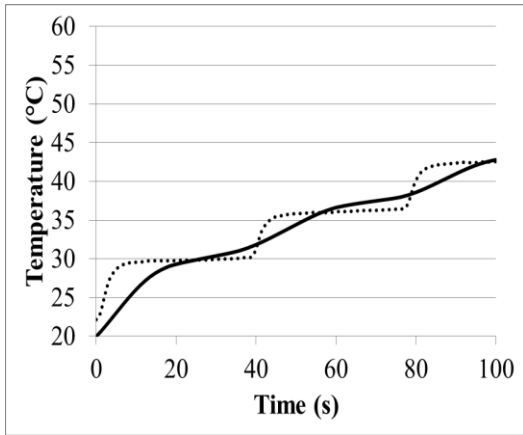
(b)



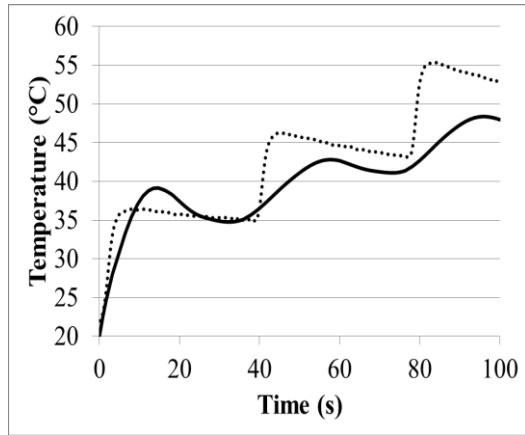
(c)

(d)

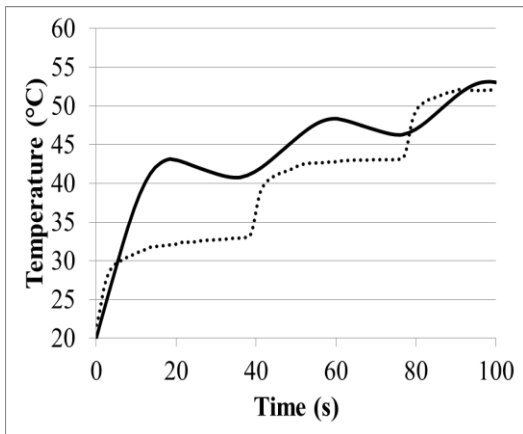
Figure 4.10 Maxwell model (line) and experimental (dotted line) results of temperature at (a) $r=10.5$ mm, (b) $r=0.0$ and (c) $r=6.1$ mm and (d) moisture content of zucchini heated by 10% microwave and 10% upper infrared power.



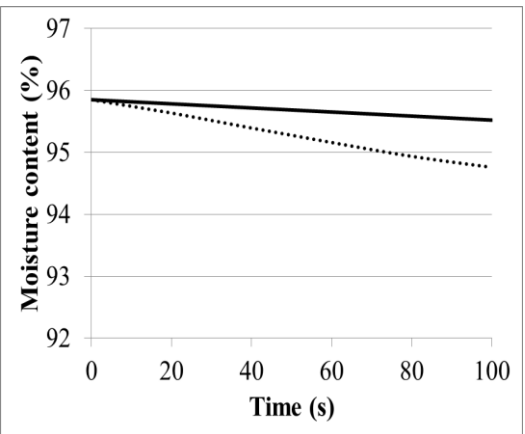
(a)



(b)

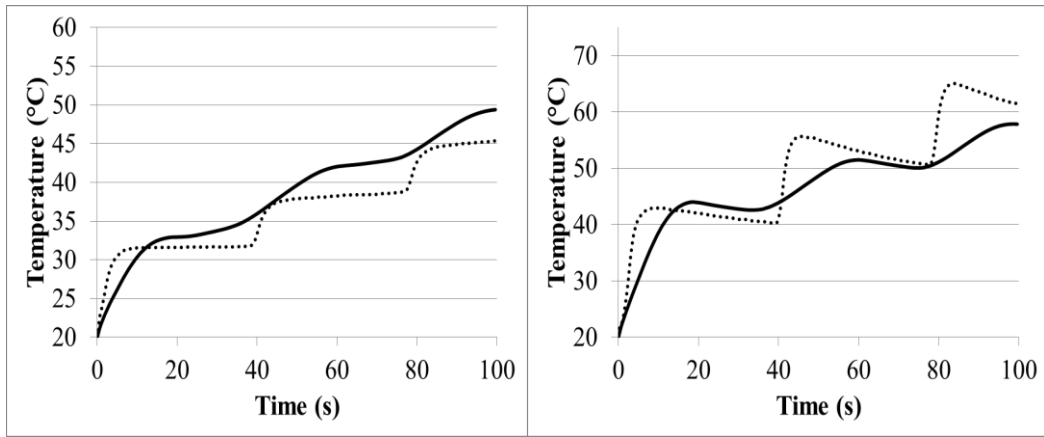


(c)



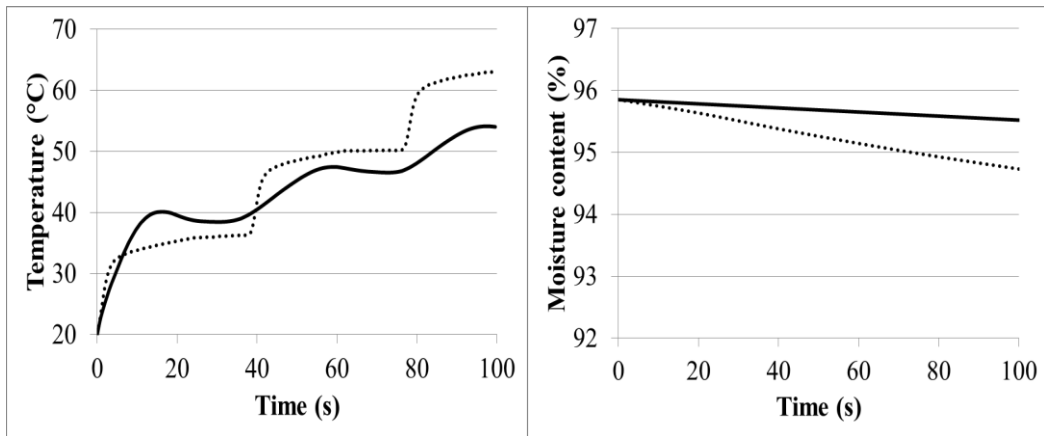
(d)

Figure 4.11 Maxwell model (line) and experimental (dotted line) results of temperature at (a) $r=10.5$ mm, (b) $r=0.0$ and (c) $r=6.1$ mm and (d) moisture content of zucchini heated by 10% microwave and 40% upper infrared power.



(a)

(b)



(c)

(d)

Figure 4.12 Maxwell model (line) and experimental (dotted line) results of temperature at (a) $r=10.5$ mm, (b) $r=0.0$ and (c) $r=6.1$ mm and (d) moisture content of zucchini heated by 10% microwave and 70% upper infrared power.

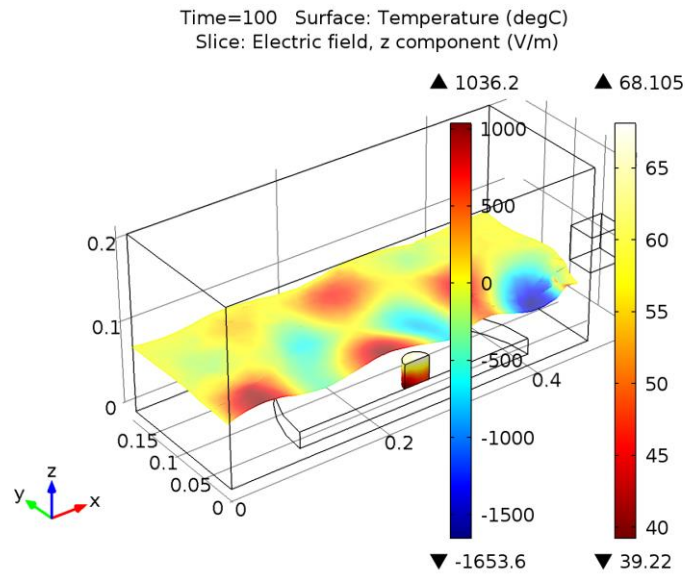


Figure 4.13 Electric field (V/m) at $z=0.08$ cm and the surface temperature of the zucchini of the zucchini at $t=100$ s

Electric field profile was obtained by using the Maxwell Equations with the initial and boundary conditions. Electric field at $z=0.08$ cm and the surface temperature of the zucchini were shown in Figure 4.13. It can be seen that the electric field inside the oven has some ups and downs, which is practically reasonable since microwave generates heat by the oscillatory movement of ions.

4.4 Effect of Microwave and Infrared Powers on Temperature Distribution and Moisture content of Zucchini

The effects of microwave and infrared power on temperature distribution and moisture content of zucchini were analyzed by showing experimental and model results obtained based on Lambert Law. Furthermore, the variation of temperature with respect to position ($r=0.0, 6.1$ and 10.5 mm) in the zucchini specimen was analyzed.

4.4.1 Effect of Microwave Power on Temperature and Moisture content of Zucchini

Figure 4.14 showed that at constant infrared power (10%) when the microwave power increased from 10% to 50%, temperature at the center of the zucchini increased rapidly. In 15 s of heating period, center temperature increased up to 98 °C for 50% microwave power while it was around to 38 °C for 10% microwave power. This can be mainly due to the difference in heating cycle times. For 10% microwave power, heating was on for 3 s and off for 37 s whereas for 50% microwave power it was 16 s on and 22 s off. Thus, for nearly 40 s period of heating by 10% microwave power, magnetron emitted energy for 3 s and by 50% microwave power it gave energy for 16 seconds. More heat was generated inside the zucchini, leading to the sudden increase in internal temperature. Similarly, Figure 4.15 showed that when microwave power level increased from 10% to 50% at 70% infrared power, temperature at $r=0.0$ (center) increased rapidly. The same trend was observed for temperatures at other positions ($r=10.5$ and $r=6.1$ mm) when the microwave power increased from 10% to 50%.

However, as it can be seen from Figure 4.16 when microwave power increased from 30% to 50% with 10% infrared power, temperature at $r=0.0$ (center) of the zucchini increased slightly. For 50% microwave power, heating was on for 16 s and off for 22 s whereas for %30 microwave power it was 14 s on- 22 s off. 2 s of heating difference did not change the temperature of the zucchini significantly. The same trend was observed for temperatures at different locations ($r=10.5$ and $r=6.1$ mm) when microwave power increased from 30% to 50%.

It was found in this study that as microwave power increased, the temperature of the food increased significantly. Almeida (2005) also showed similar result. Almeida (2006) revealed that there was 67% increase in the temperature of the surface of the food as heat flux increased from level 1 to 5. From level 5 to 10, this increase was not so significant since there was a 2 s of increase in heating time.

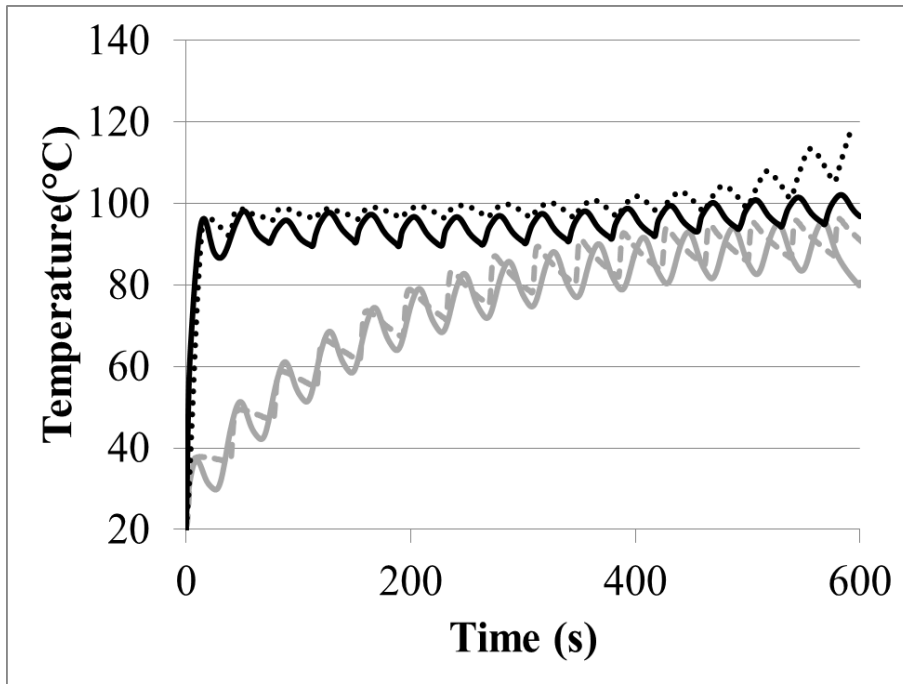


Figure 4.14 Lambert model (line) and experimental (dotted line) results of temperature at the center ($r=0.0$) of the zucchini heated by 10% infrared and 50% microwave (black) and 10% infrared and 10% microwave power (gray)

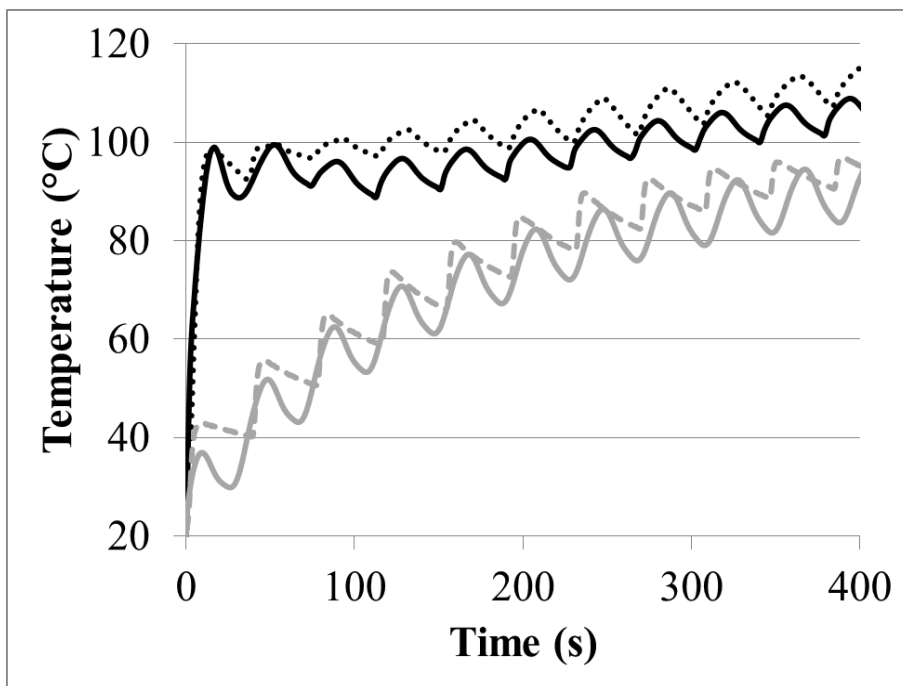


Figure 4.15 Lambert model (line) and experimental (dotted line) results of temperature at the center ($r=0.0$) of the zucchini heated by 70% infrared and 50% microwave (black) and 70% infrared and 10% microwave power (gray)

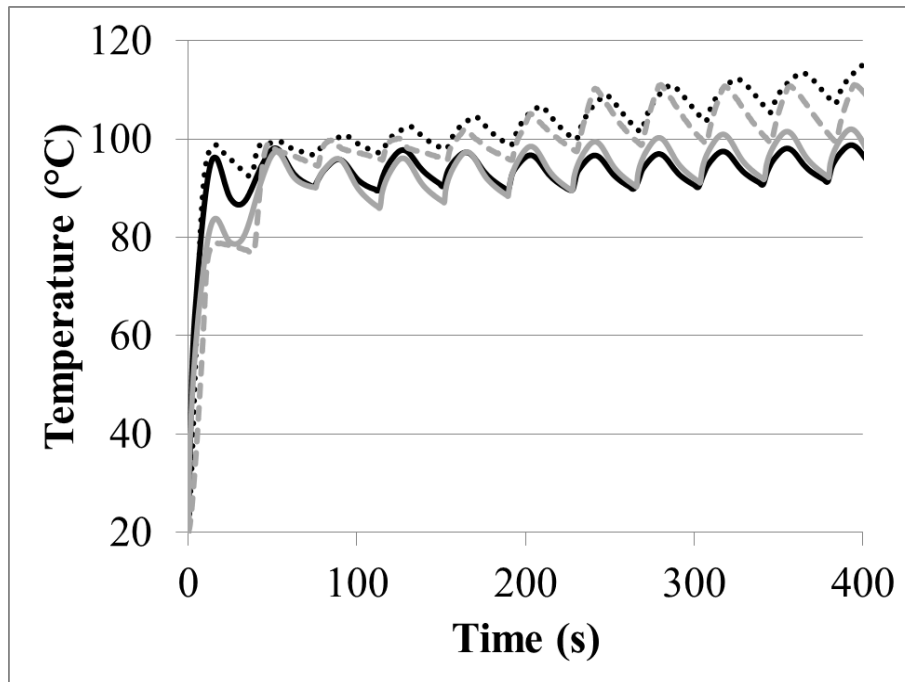


Figure 4.16 Lambert model (line) and experimental (dotted line) results of temperature at the center ($r=0.0$) of the zucchini heated by 10% infrared and 50% microwave (black) and 10% infrared and 30% microwave power (gray)

It can be seen from Figure 4.17 that using 50% microwave and %10 infrared power, moisture content decreased from 95.85% to 58.7%. However, with 10% microwave and %10 infrared power, moisture content decreased slightly from 95.85% to 94.2%. Thus, when microwave power increased from 10% to 50% with 10% infrared power, moisture removal rate of zucchini was increased significantly. Similar result was observed when microwave power increased from 10% to 50% with 70% infrared power as can be seen in Figure 4.18.

It was concluded in this study that as microwave power increased, the moisture content of the zucchini decreased. Internal heating of microwaves resulted in generation of pressure gradient of vapor from the interior to the surface of the product. As microwave power increased the interior pressure increased leading to more moisture flow from the food. Shivhare et al. (1992) dried corn by microwave and hot air and concluded that when the magnitude of microwave power increased

the drying rate increased. In another study of Wang and Xi, (2005) it was found that at high microwave power moisture transfer occurred rapidly from the center to the surface as a result of the generation of more heat. Hu et al. (2006, 2007) found that the drying time was reduced with an increase in microwave power level.

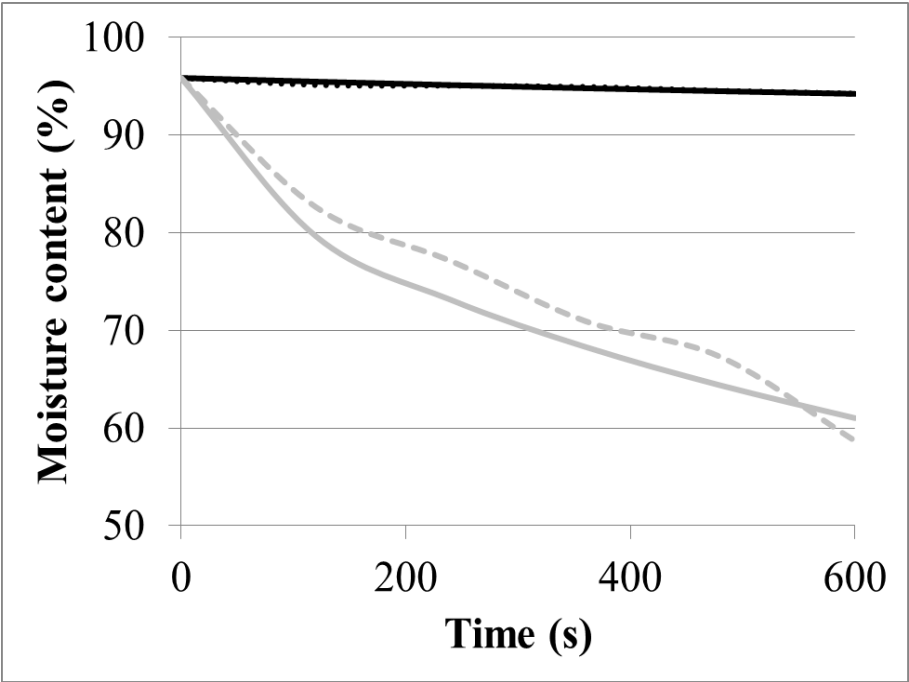


Figure 4.17 Lambert model (line) and experimental (dotted line) results of moisture content of the zucchini heated by 10% infrared and 50% microwave (gray) and 10% infrared and 10% microwave power (black)

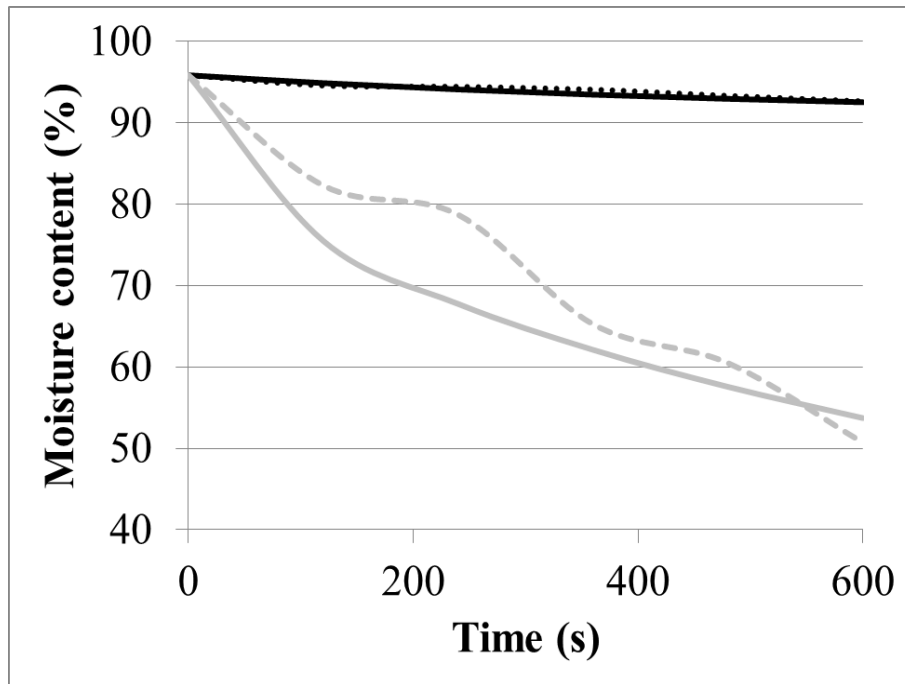


Figure 4.18 Lambert model (line) and experimental (dotted line) results of moisture content of the zucchini heated by 70% infrared and 50% microwave (gray) and 70% infrared and 10% microwave power (black)

4.4.2 Effect of Infrared Power on Temperature and Moisture content of Zucchini

It can be seen from Figure 4.19 that as infrared power increased, temperature of the zucchini increased. The same trend was observed for temperatures at $r=0.0$ and $r=6.1$ mm when the infrared power increased from 10% to 70%.

Similarly, there was a slight increase in the temperature at $r=10.5$ mm of the zucchini when infrared power increased from 10% to 70% at 30% microwave power (Figure 4.20). When infrared power increased from 10% to 40% at 50% microwave power, there was no significant change in the temperature at $r=0.0$ (Figure 4.21). The same trends were observed when temperatures were measured at different locations.

It was found in this study that as infrared power increased, the temperature of the food increased. However, the increase in temperature with infrared power was not as much as the case in increasing microwave power, since microwave heating

dominated the combination heating process. Tireki et al. (2006b) also found that microwave heating was the dominant mechanism affecting moisture loss in microwave-infrared drying.

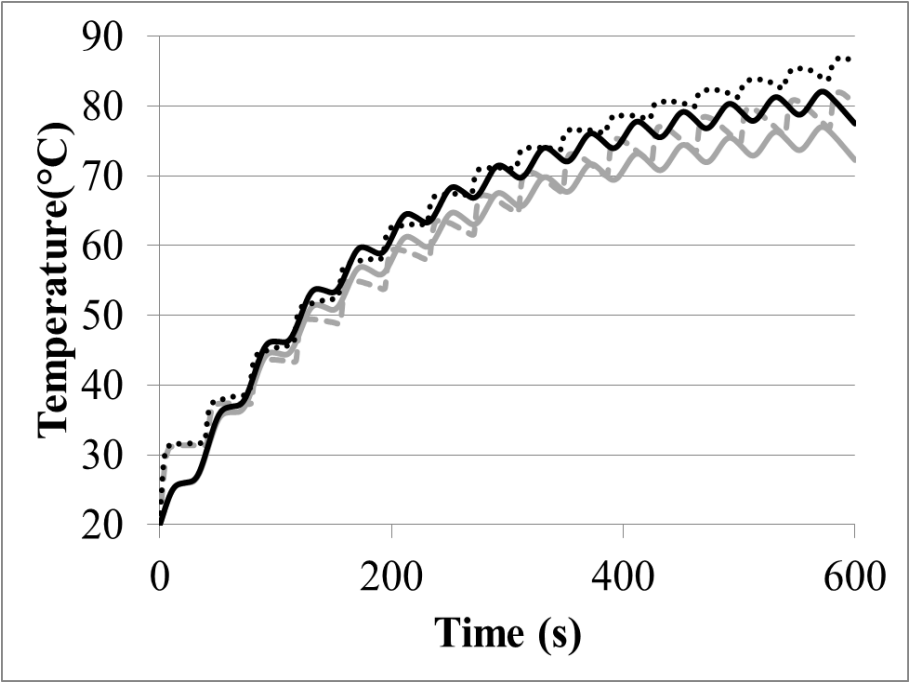


Figure 4.19 Lambert model (line) and experimental (dotted line) results of temperature at $r=10.5$ mm of the zucchini heated by 70% infrared power and 10% microwave power (black) and 10% infrared power and 10% microwave power (gray)

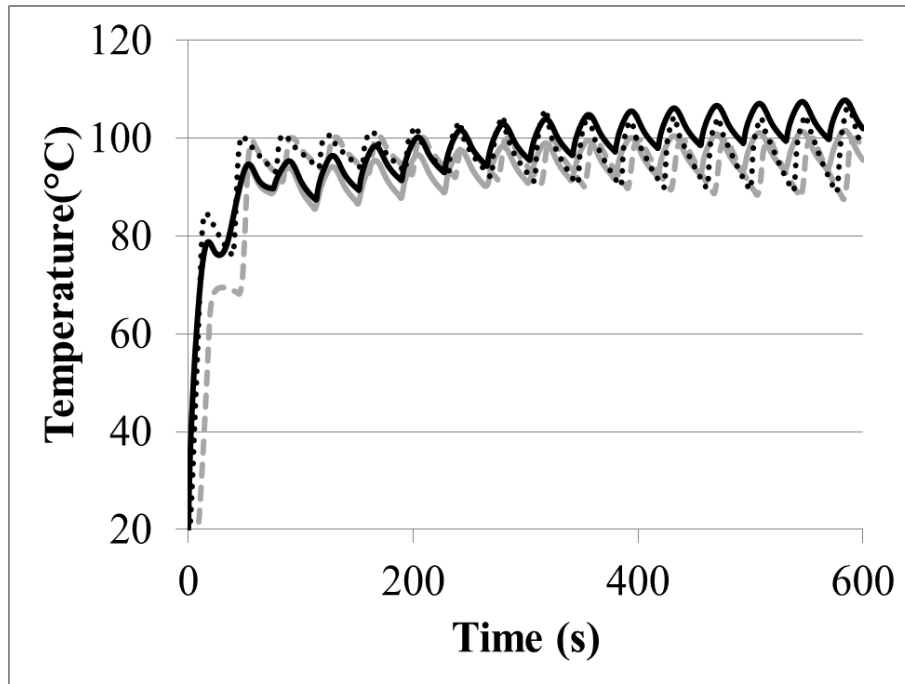


Figure 4.20 Lambert model (line) and experimental (dotted line) results of temperature at $r=10.5$ mm of the zucchini heated by 70% infrared power and 30% microwave power (black) and 10% infrared power and 30% microwave power (gray)

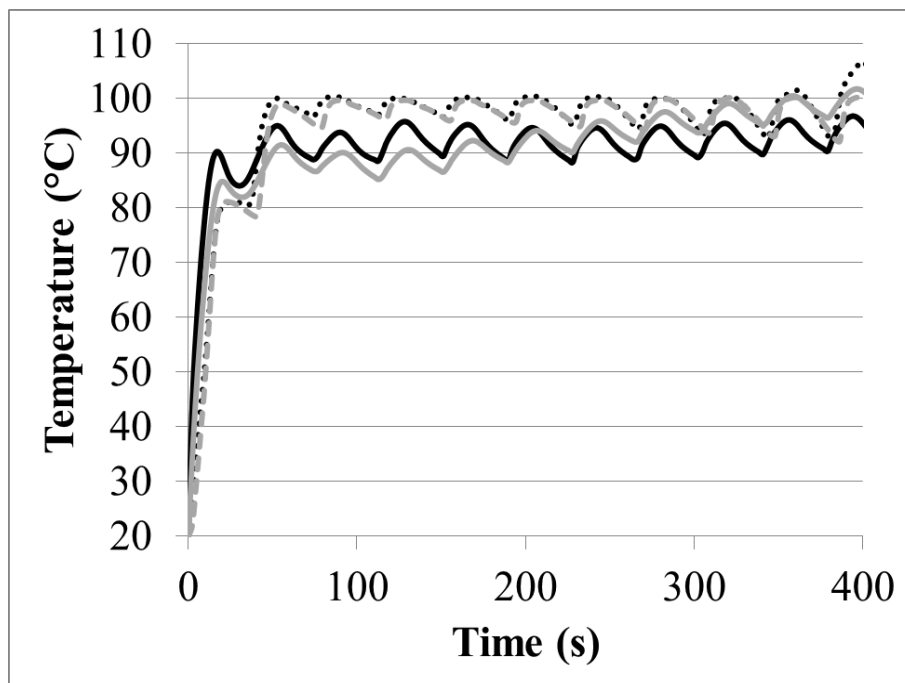


Figure 4.21 Lambert model (line) and experimental (dotted line) results of temperature at $r=10.5$ of the zucchini heated by 40% infrared power and 50% microwave power (black) and 10% infrared power and 50% microwave power (gray)

When infrared power increased from 10% to 70% at 10% microwave power, in 600 s heating time, moisture content decreased to 94.25% and 92.5% respectively (Figure 4.22). Whereas when infrared power increased from 10% to 70% with 30% microwave power, moisture content decreased to 78.83% and 65.76%, respectively (Figure 4.23).

It was concluded in this study that as microwave power increased, the moisture content of the zucchini decreased. Since, microwave power dominated the heating process, moisture removal did not increase with infrared power as much as with microwave power. Wang and Sheng, (2006) found that the dehydration rate increased with infrared power level at the same moisture content. It was concluded that the mass transfer rate was more rapid with the higher power settings since more heat was generated within the food. Datta (2007b) and Sharma (2005) both stated that as infrared power increased, the surface moisture removal increased.

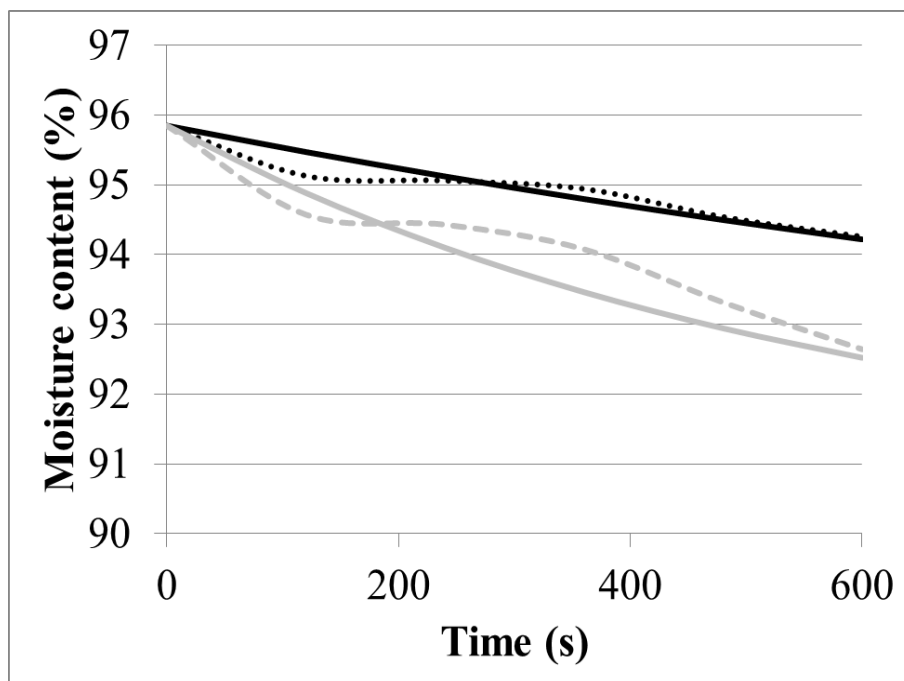


Figure 4.22 Lambert model (line) and experimental (dotted line) results of moisture content of the zucchini heated by 70% infrared power and 10% microwave power (gray) and 10% infrared power and 10% microwave power (black)

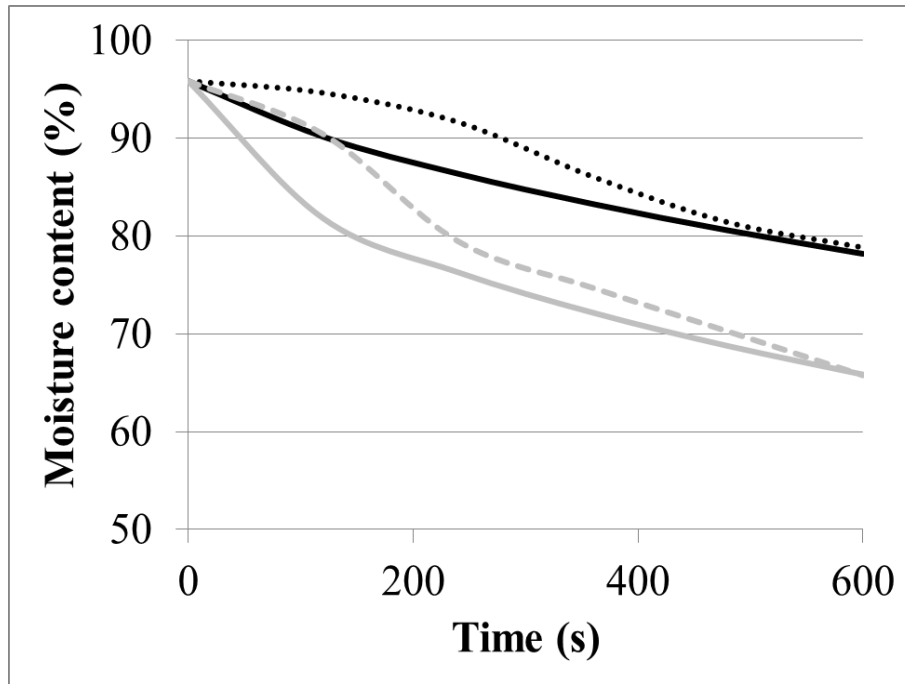


Figure 4.23 Lambert model (line) and experimental (dotted line) results of moisture content of the zucchini heated by 70% infrared power and 30% microwave power (gray) and 10% infrared power and 30% microwave power (black)

4.4.3 Variation of Temperature with Respect to Position in Zucchini

Temperature measurement was done at different positions of the zucchini such as: $r=0.0$, 6.1 and 10.5 mm. Probes positioned at $r=10.5$ mm and $r=0.0$ was placed such that the midpoint temperature of the sample could be measured whereas probe at $r=6.1$ mm could measure surface temperature.

Figure 4.24 shows the experimental data and model for the temperature at $r=0.0$ and $r=10.5$ mm of the zucchini heated by 10% microwave and 10% infrared power. The center temperature was higher than the temperature at $r=10.5$ mm of the zucchini because of internal heating and focusing effect of microwaves. Chamchong and Datta (1999b) stated that cylinders were the second best shape for microwave heating, after spheres since heating could be concentrated in cylinder due to their curvatures. These curvatures could focus the microwave heating and provide a much higher electric field inside. Gunasekaran and Yang (2007) found that for 3.5 cm

radius samples, there were more focusing power at the radial center. Lin et al. (1995) predicted the temperature distribution in agar gels and found that in cylindrical samples center temperature was higher than those at other locations within the cylinder which was similar to the results found in this study. According to Yang and Gunasekaran (2004) the location of power focusing depended on the sample size, and was not necessarily at the center for a very large sample.

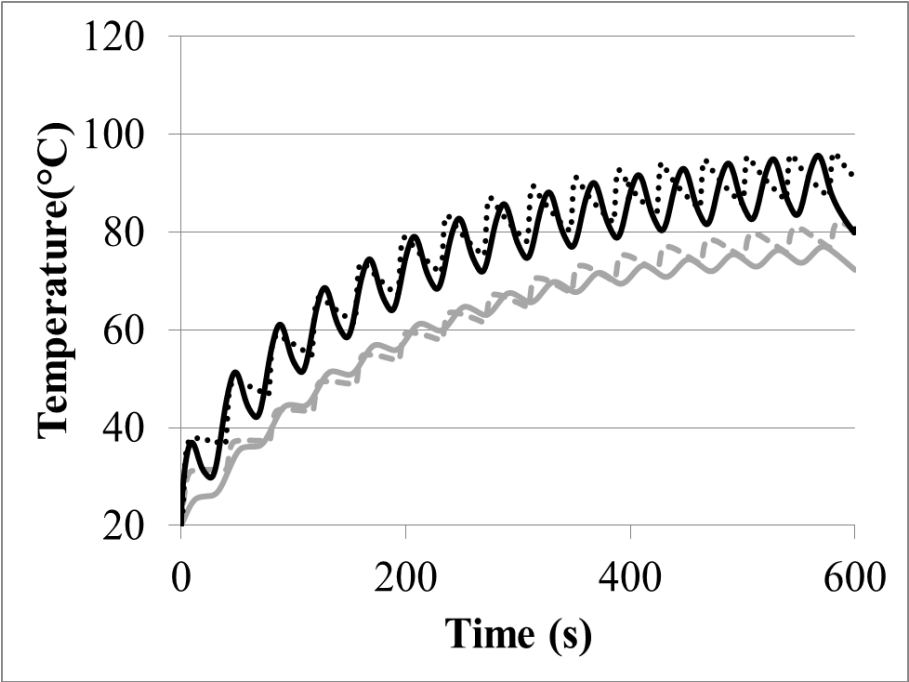


Figure 4.24 Lambert model (line) and experimental (dotted line) results of temperature of the zucchini heated by 10% infrared and 10% microwave power at $r=0.0$ (black) and $r=10.5$ mm (gray).

Figure 4.25 showed that at 10% microwave and 40% infrared power, temperature at $r=0.0$ was slightly higher than the temperature at $r=6.1$ mm which was positioned so as to measure surface temperature. Surface temperature was as high as center temperature because of surface heating property of infrared heating.

It was concluded that temperature at $r=0.0$ (center) and $r=6.1$ mm (surface) of the zucchini was higher than the temperature at $r=10.5$ mm. Microwave’s internal heating increased the center temperature while infrared’s surface heating increased the surface temperature. Campanone (2005) also stated that in cylinders, microwaves

generated non uniform radial distribution. Thus, surface and center temperatures reached the highest values.

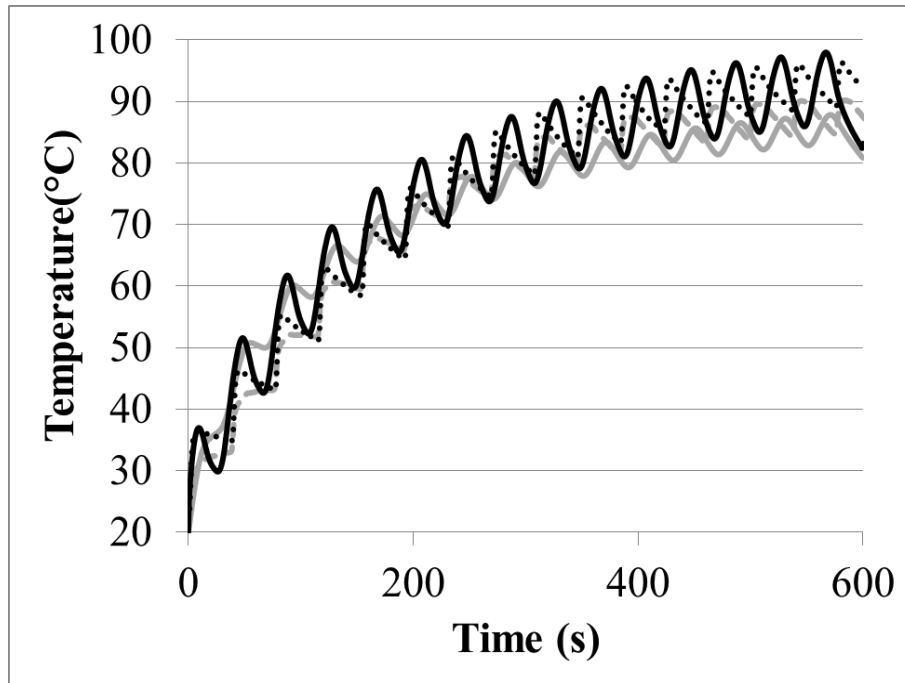


Figure 4.25 Lambert model (line) and experimental (dotted line) results of temperature of the zucchini heated by 40% infrared power and 10% microwave power at $r=0.0$ (black) and $r=6.1$ (gray)

4.4.4 Variation of Moisture Content with Respect to Position in Zucchini

It can be seen from Figure 4.26 that moisture content data obtained based on Lambert Law changed with respect to r and z directions and moisture was lost through surface, significantly. Furthermore, as microwave power increased from 10% to 50%, more moisture was pumped from the inside through the surface.

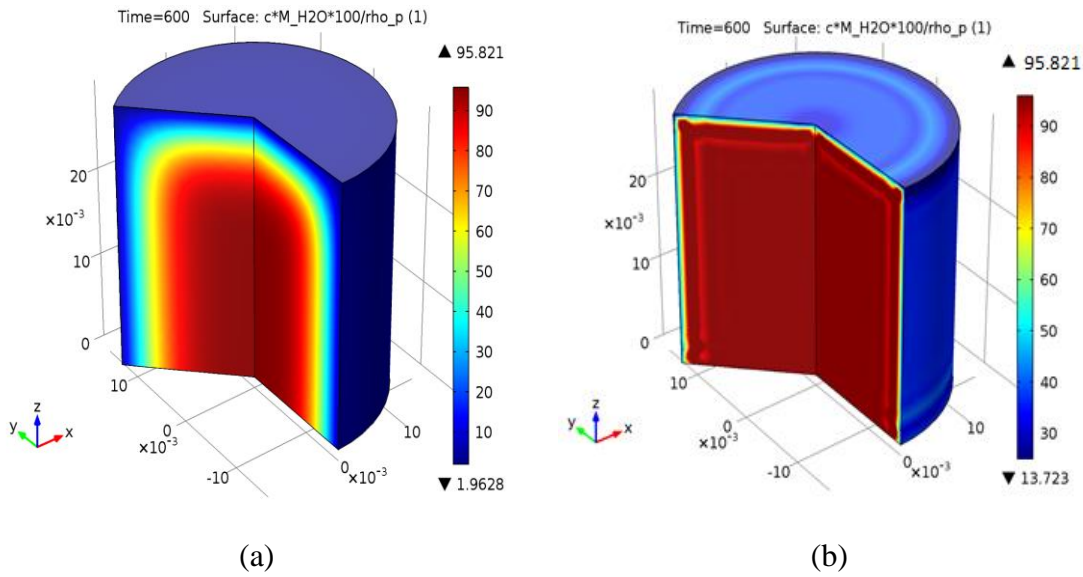
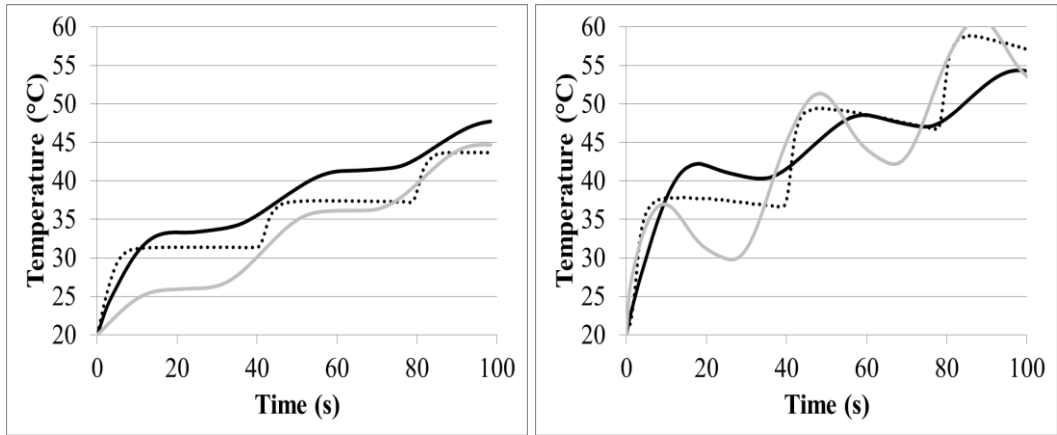


Figure 4.26 Simulation moisture content data when (a) 70% infrared and 50% microwave, (b) 70% infrared and 10% microwave power were selected for 600 s heating time.

4.5 Comparison of Models Based on Maxwell Equations and Lambert Law

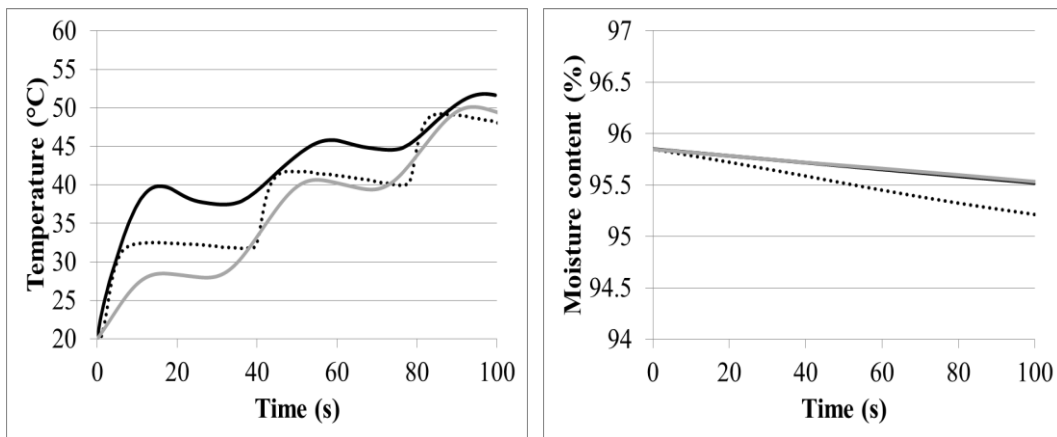
Figures 4.27-4.29 show the variation of temperature and moisture content of zucchini during heating in microwave-infrared combination oven at different power levels. Experimental data and models based on Maxwell Equations and Lambert Law for different microwave and infrared powers for 100 s heating period were given. Temperatures were given for different positions of the zucchini such as $r=0.0$, 6.1 and 10.5 mm.

Root Mean Square Errors (RMSE) of Lambert and Maxwell models obtained for different operating conditions of the oven and positions of the temperature probe within the zucchini were presented in Table 4.6. RMSE of Lambert and Maxwell models obtained for moisture content were tabulated in Table 4.7.



(a)

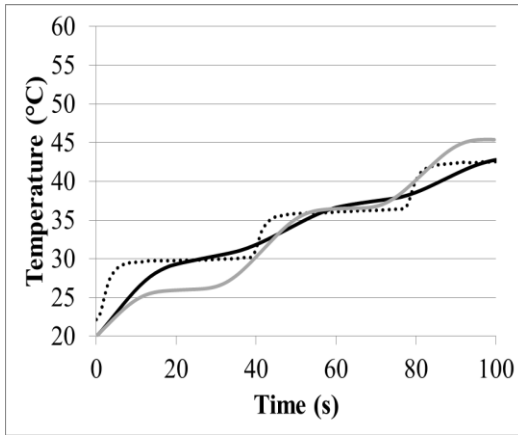
(b)



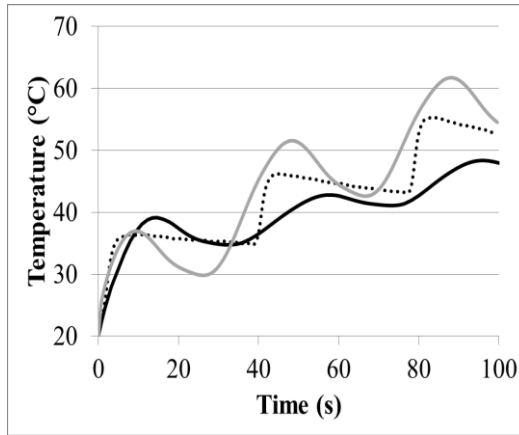
(c)

(d)

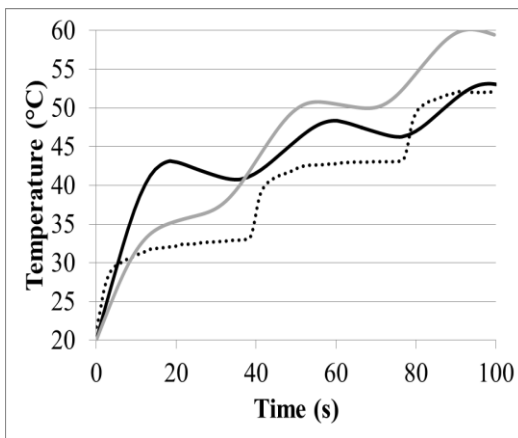
Figure 4.27 Maxwell Model (black line), Lambert Model (gray line) and experimental (dotted line) results of temperature at (a) $r=10.5$ mm, (b) $r=0.0$ and (c) $r=6.1$ mm (surface) of the zucchini and (d) moisture content of zucchini heated by 10% microwave power and 10% upper infrared power for 100 s.



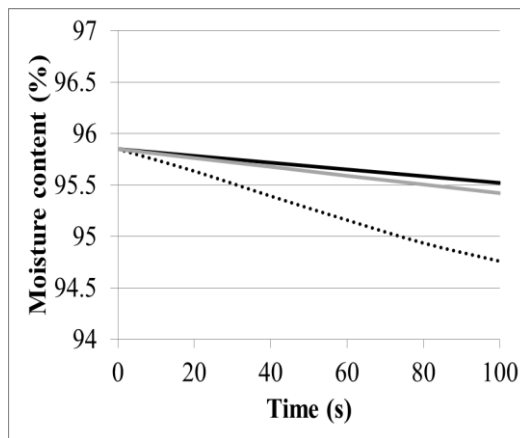
(a)



(b)



(c)



(d)

Figure 4.28 Maxwell Model (black line), Lambert Model (gray line) and experimental (dotted line) results of temperature at (a) $r=10.5$ mm, (b) $r=0.0$ and (c) $r=6.1$ mm (surface) probes of the zucchini and (d) moisture content of zucchini heated by 10% microwave power and 40% upper infrared power for 100 s.

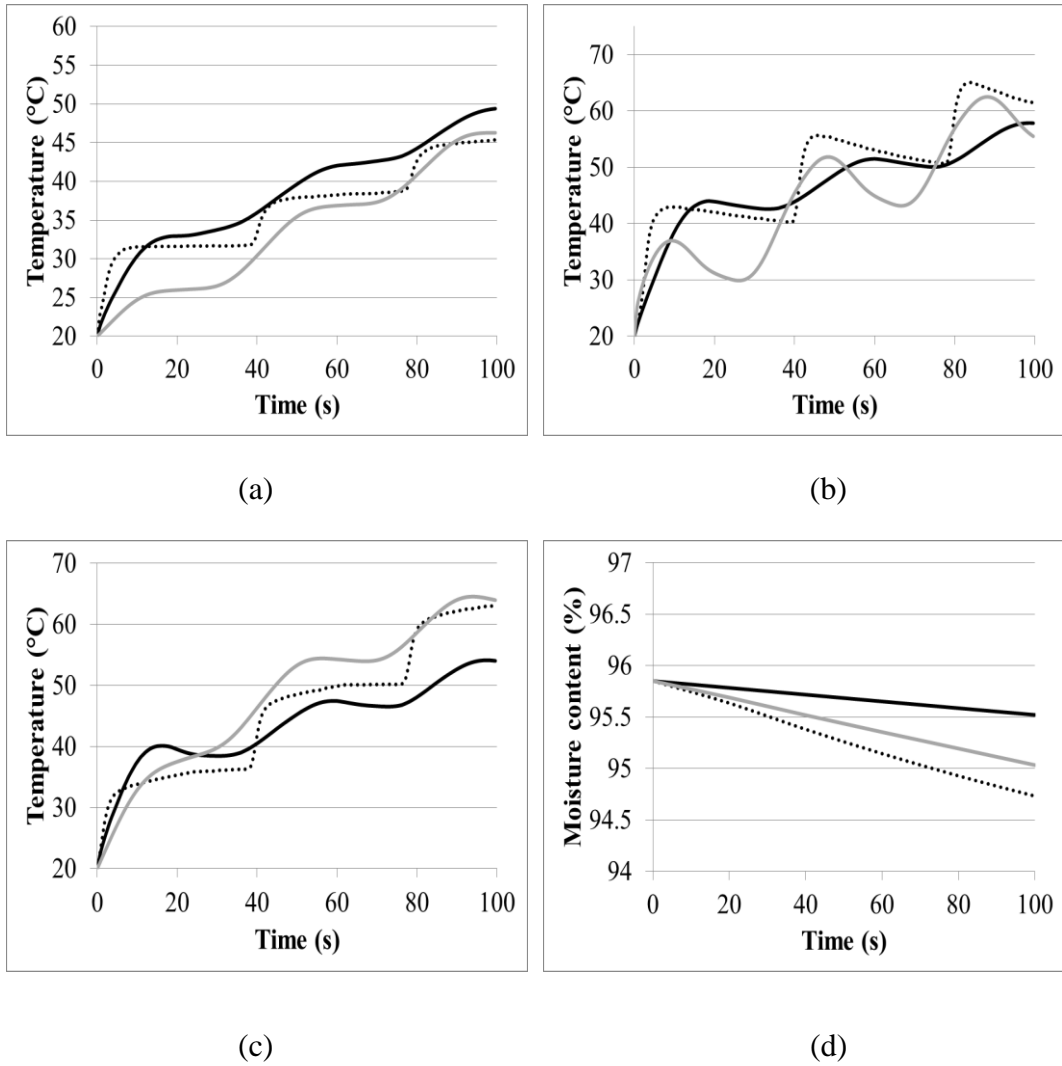


Figure 4.29 Maxwell Model (black line), Lambert Model (gray line) and experimental (dotted line) results of temperature at (a) $r=10.5$ mm, (b) $r=0.0$ and (c) $r=6.1$ mm (surface) probes of the zucchini and (d) moisture content of zucchini heated by 10% microwave power and 70% upper infrared power for 100 s.

Table 4.6 Root Mean Square Errors (RMSE) of Lambert and Maxwell models obtained for different microwave (MWP) and infrared powers (IRP) and positions of the temperature probe

MWP (%)	IRP (%)	Position of the Temperature Probe	Lambert Model	Maxwell Model
10	10	r=10.5 mm	3.57	2.96
10	10	r=0.0 mm	3.91	3.94
10	10	r=6.1 mm	2.92	4.39
10	40	r=10.5 mm	2.80	1.97
10	40	r=0.0 mm	4.30	4.60
10	40	r=6.1 mm	6.21	5.77
10	70	r=10.5 mm	3.87	2.85
10	70	r=0.0 mm	6.47	5.40
10	70	r=6.1 mm	3.77	5.51

Table 4.7 Root Mean Square Errors (RMSE) of Lambert and Maxwell models obtained for moisture content predictions for different microwave (MWP) and infrared powers (IRP)

MWP (%)	IRP (%)	Lambert Model	Maxwell Model
10	10	0.2000	0.1900
10	40	0.4200	0.4800
10	70	0.0005	0.4900

As it can be seen from Table 4.6, Maxwell models gave generally better results than Lambert model for different operating conditions and positions of the temperature probe except for 10% MWP-10%MWP at r=6.1 mm and 10% MWP-70%MWP at r=6.1 mm.

Yang et al. (2004) applied pulsed and continuous microwave energy to agar gel cylinders. Measured temperature values were compared with model results based on Lambert's Law and Maxwell Equations. Models of Maxwell Equations gave wave effect inside the sample however, Lambert's law did not. It was concluded that Maxwell's equations provided statistically more accurate results than the Lambert's law, especially around the edge of sample.

It has been concluded that Lambert's law gave comparable results with the experimental data (Liu et al., 2005). However, it was not a good way of representing exact microwave power distribution (Datta et al., 2001). In literature, the Maxwell's and Lambert's law were compared by several studies to predict temperature distribution of model food during microwave heating (Yang and Gunasekaran, 2004, Liu et al., 2005). Yang and Gunasekaran, (2004) stated that using Maxwell's equations to predict electromagnetic distribution was more accurate than Lambert's law.

Ayappa et al. (1991) stated that the exponentially decaying energy assumption for power estimation was only valid for semi-infinite slabs. Critical thickness of the slab above which the Lambert approximation was valid was 2.7 times the penetration depth. However, in this study it was proven that the numerical predictions based on Lambert Law could give proper results like predictions obtained by Maxwell Equations for small scale cylindrical foods since the exact form of microwave power source term derived by Lin et al (1995) was used. Zhou et al. (1995) also found that the Lambert's Law could be correctly used for cylindrical domain by rewriting the power term by taking the decreasing control volume into account. Power in this case was concentrated along the central axis.

Similarly, it can be seen from Table 4.7 that for the zucchini heated in microwave infrared combination oven for 100 s, predictions for moisture content based on Lambert and Maxwell Equations were comparable.

CHAPTER 5

CONCLUSION AND RECOMMENDATIONS

Modeling heat and mass transfer in food is a challenging topic. There is no information in literature about modeling of zucchini during heating in microwave-infrared combination oven. Thus, it was not possible to find data especially about heat and mass transfer parameters for zucchini.

Models based on Lambert Law were in good agreement with the measured data. RMSE values were ranging from 2.44 to 9.37 and from 0.16 to 5.68 for temperature and moisture content, respectively.

Maxwell models gave better results than Lambert model for different operating conditions and positions of temperature. RMSE ranged from 1.97 to 5.77 for temperature while RMSE for moisture content ranged from 0.19 to 0.49.

Incident surface power (P_0) and moisture diffusion coefficient (D) were found to be directly related to microwave power. They were modelled as a function of microwave power with high coefficient of determination values. Whereas, mass transfer coefficient (k_c) found to be changed by microwave and infrared powers and was modelled as a function of microwave (%MWP) and infrared power (%IRP) with high coefficient of determination value.

It was found in this study that as microwave and infrared powers increased, the temperature increased and the moisture content of the food decreases significantly. However, temperature did not increase with infrared power as much as with microwave power since microwave heating dominated the combination heating

process. Similarly, rate of moisture removal did not increase with infrared power as much as with microwave power.

Microwave's internal heating and focusing effect increased the center temperature and infrared's surface heating effect increased the surface temperature.

For future work, it is recommended to apply the models developed in this study on other foods with different dielectric properties to examine the heating mechanism of microwave-infrared oven further. It is also recommended to apply the models for foods in different shapes to examine whether these models were applicable or not.

REFERENCES

- Abe T, Afzal TM. 1997. Thin-layer infrared radiation drying of rough rice. *J Agric Eng Res* 67:289–97.
- Afzal TM, Abe T, Hikida Y. 1999. Energy and quality aspects of combined FIR convection drying of barley. *J Food Eng* 42:177–82.
- Afzal TM, Abe T. 1998. Diffusion in potato during far infrared radiation drying. *J Food Eng* 37(4):353–65.
- Al-Duri, B., and McIntyre, S. (1992). Comparison of drying kinetics of foods using a fan-assisted convection oven, a microwave oven and a combined microwave convection oven. *Journal of Food Engineering*, 15, 139–155.
- Ali S.D., Ramaswamy H.S., and Awuah G.B. (2002) “Thermo-Physical Properties Of Selected Vegetables As Influenced By Temperature And Moisture Content” *Journal of Food Process Engineering* 25 417-433.
- Almeida M.F. (2005) Modeling Infrared and Combination Infrared-Microwave Heating of Foods in an Oven. PhD thesis. Cornell University.
- AOAC. (1984). Official methods of analysis (14th ed.). Association of Official Analytical Chemists, Washington, DC
- Ayappa, K. G., Davis, H. T., Crapiste, G., Davis, E. A. and Gordon, J. (1991). Microwave heating: an evaluation of power formulations. *Chem. Engng Sci.*, 46 (4), 1005- 16.

Aydogdu A. and Sumnu G. and Sahin S., (2015) Effects of Microwave-Infrared Combination Drying on Quality of Eggplants Food Bioprocess Technol 8:1198–1210.

Barba A. A and D'Amore M., (2012) Relevance of Dielectric Properties in Microwave Assisted Processes. Microwave Materials Characterization. InTech. 6th Chapter. 91-117.

Bilbao-Sainz, C., Andres, A., Chiralt, A., and Fito, P. (2006). Microwaves phenomena during drying of apple cylinders. Journal of Food Engineering, 74(1), 160–167.

Bouraout, M., Richard, P., and Durance, T. (1994). Microwave and convective drying of potato slices. Journal of Food Process Engineering, 17, 353±363.

Campanone, L.A., Zaritzky, N.E., 2005. Mathematical analysis of microwave heating process. Journal of Food Engineering 69 (3), 359–368.

Chamchong, M., Datta, A.K., 1999a. Thawing of foods in a microwave oven: I. Effect of power levels and power cycling. Journal of Microwave Power and Electromagnetic Energy 34 (1), 9–21.

Chamchong, M., Datta, A.K., 1999b. Thawing of foods in a microwave oven: II. Effect of load geometry and dielectric properties. Journal of Microwave Power and Electromagnetic Energy 34 (1), 22–32.

Chen, A. A., Singh, R. K., Haghghi, K., and Nelson, P. E. (1993). Finite element analysis of temperature distribution in microwave cylindrical potato tissue. Journal of Food Engineering, 18, 351–368.

Chen, D., Haghghi, K., Singh, R. K. and Nelson, P. E. (1990). Finite element analysis of temperature distribution during microwaved particulate foods. ASAE Paper No. 906602. St Joseph, MI.

Chen H., Marks B. P, Murphy R. Y. (1999). Modeling coupled heat and mass transfer for convection cooking of chicken patties . *Journal of Food Engineering*. 42. 139-146

Chen J., Pitchai K., Birla S., Negahban M., Jones D., Subbiah J. (2014). Heat and mass transport during microwave heating of mashed potato in domestic oven--model development, validation, and sensitivity analysis. *J Food Sci*. 79(10):E1991-2004

Curet S., Rouaud O., Boillereaux L. (2014) “Estimation of Dielectric Properties of Food Materials During Microwave Tempering and Heating”. *Food Bioprocess Technol*. 7:371–384.

Das I, Das SK, Bal S. 2004. Drying performance of a batch type vibration-aided infrared dryer. *J Food Eng* 4:129–33.

Datta, A. K. (1990). Heat and mass transfer in the microwave processing of food. *Chem. Engng Progress*, 6,47-53.

Datta, A. K. (2007a). Porous media approaches to studying simultaneous heat and mass transfer in food processes. I: Problem formulations. *Journal of Food Engineering*, 80, 80–95.

Datta, A. K. (2007b). Porous media approaches to studying simultaneous heat and mass transfer in food processes. II: Property data and representative results. *Journal of Food Engineering*, 80, 96–110.

Datta, A. K., and Anantheswaran, R. C. (2001). *Handbook of microwave technology for food applications*. New York: Dekker Inc.

Datta, A. K., and H. Ni. 2002. Infrared and hot air-assisted microwave heating of foods for control of surface moisture. *Journal of Food Engineering* 51: 355–364.

Datta, A. K., and Ni, H. (1999). Infrared and hot air additions to microwave heating of foods for control of surface moisture. *Journal of Food Engineering*, 51, 355–364.

Decareau, R.V., 1992. *Microwave Foods: New Product Development*. Food Nutrition Press Inc., Connecticut.

Dostie M, Seguin JN, Maure D, Tonthat QA, Chatingy R. 1989. Preliminary measurements on the drying of thick porous materials by combinations of intermittent infrared and continuous convection heating. In: Mujumdar AS, Roques MA, editors. *Drying'89*. New York: Hemisphere Press.

Drouzas, A. E., and Saravacos, G. D. (1999). Microwave/vacuum drying of model fruit gels. *Journal of Food Engineering*, 39, 117–122.

Feng, H., Tang, J., and Dixon-Warren, S. J. (2000). Determination of moisture diffusivity of red delicious apple tissues by thermogravimetric analysis. *Drying technology*, 18, 1183–1199.

Feng, H., Tang, J., Cavalieri, R. P., and Plumb, O. A. (2001). Heat and mass transport in microwave drying of porous materials in a spouted bed. *AICHE Journal*, 47, 1499–1511.

Fenton GA, Kennedy MJ. 1998. Rapid dry weight determination of kiwifruit pomace and apple pomace using an infrared drying technique. *New Zealand J Crop Horti Sci* 26: 35–8.

Funebo, T., and Ohlsson, T. (1998). Microwave-assisted air dehydration of apple and mushroom. *Journal of Food Engineering*, 38, 353±367.

Funebo T, Ohlsson T. 1999. Dielectric properties of fruits and vegetables as a function of temperature and moisture content. *J Micro Pow EE* 34(1):42-54.

Giese, J. 1992. Advances in microwave food processing. *Food Technology*, 46 (9), 118-123.

Gunasekaran S., Yang H. (2007) Effect of experimental parameters on temperature distribution during continuous and pulsed microwave heating. *Journal of Food Engineering* 78 1452–1456

Haldera A., Datta A.K. (2012). Surface heat and mass transfer coefficients for multiphase porous media transport models with rapid evaporation. *food and bioproducts processing*. 90. 475–490

Hallstrom, B., (1979). Heat and mass transfer in industrial cooking. *Food Process Engineering* 1, 457–465

Hellebrand H, Beuche H, Linke M. (2001). Determination of Thermal Emissivity and Surface Temperature Distribution of Horticultural Products. 6th Intl. Symposium on Fruit, Nut and Vegetable Production Engineering, Potsdam, Germany; 2001 Sep 11-4 (2001)

Hu, Q. -G., Zhang, M., Mujumdar, A. S., Xiao, G. -N., & Sun, J. -C. (2006). Drying of edamames by hot air and vacuum microwave combination. *Journal of Food Engineering*, 77, 977–982.

Hu, Q. -G., Zhang, M., Mujumdar, A. S., Xiao, G. -N., & Sun, J. -C. (2007). Performance evaluation of vacuum microwave drying of edamame in deep-bed drying. *Drying Technology*, 25, 731–736

Jaturonglumlert, S., and Kiatsiriroat, T. (2010). Heat and mass transfer in combined convective and far-infrared drying of fruit leather. *Journal of Food Engineering*, 100:254-260.

Jun, S., Krishnamurthy, K., Irudayaraj, J., & Demirci, A. (2011). Fundamentals and Theory of Infrared Radiation. In Z. Pan, & G. G. Atungulu, *Infrared Heating for Food and Agricultural Processing* (pp. 1-18). Boca Raton: CRC Press.

Kadlec, P., Rubecova, A., Hinkova, A., Kaasova, J., Bubnik, Z. and Pour, V. (2001). Processing of yellow pea by germination, microwave treatment and drying. *Innovative Food Science and Emerging Technologies*, 2, 133–137.

Khair, R., Z. Pan, A. Salim, B.R. Hartsough, and S. Mohamed. 2011. Moisture diffusivity of rough rice under infrared radiation drying. *LWT – Food Science and Technology*. 44(4):1126-1132.

Khraisheh, M.A.M., Cooper, T.J.R., Magee, T.R.A., 1997. Microwave and air drying I. Fundamental considerations and assumptions for the simplified thermal calculations of volumetric power absorption. *Journal of Food Engineering* 33 (1–2), 207–219.

Kim, S. S., and Bhowmik, S. R. (1995). Effective moisture diffusivity of plain yogurt undergoing microwave vacuum drying. *Journal of Food Engineering*, 24, 137±148.

Krishnamoorthy P. (2011)“Electromagnetic and Heat Transfer Modeling of Microwave Heating in Domestic Ovens” Theses in Food Science and Technology.

Lampinen, M. J., Ojala, K. T., and Koski, E. (1991). Modelling and measurements of infrared dryers for coated paper. *Drying Technology*, 9(4):973-1017.

Land, C. M. (2012). *Drying in the Process Industry*. New Jersey: John Wiley and Sons, Inc.

Lin, T. M., Durance, T. D., and Scaman, C. H. (1998). Characterization of vacuum microwave air and freeze dried carrot slices. *Food Research International*, 4, 111–117.

Lin, Y. E., Anantheswaran, R. C. and Puri, V. M. (1995). Modeling temperature distribution during microwave heating. *Journal of Food Engineering*. 25. 85-112

Liu, C.M., Wang, Q.Z., Sakai, N., 2005. Power and temperature distribution during microwave thawing, simulated by using Maxwell's equations and Lambert's law. *International Journal of Food Science and Technology* 40 (1), 9–21.

Malafrente L., Lamberti G., Barba A. A., Raaholt B, Holtz E., Ahrné L., (2012) “Combined convective and microwave assisted drying: Experiments and modeling”. *Journal of Food Engineering*, 112, 304–312.

Masamura, A., Sado, H., Honda, T., Shimizu, M., Nabethani, H., Hakajima, M., and Watanabe, A. (1988). Drying of potato by far infrared radiation. *Nippon Shokuhin Kogyo Gakkaishi*, 35, 309–314.

Mehinger E.; D. and Mueller G.A. Zohm, H.; Kasper. (2000) Thermal processing of silicon wafers with microwave co-heating. *Microelectronic Engineering*, 54(3-4):247

Mongpreneet S, Abe T, Tsurusaki T. 2002. Accelerated drying of welsh onion by far infrared radiation under vacuum conditions. *J Food Eng* 55:147–56.

Mudgett, R. E. (1986). Microwave properties of heating characteristics of foods. *Food Technol.*, 2,121-35.

Namiki, H., Niinuma, K., Takemura, M., and Tou, R. (1996). Effects of far-infrared irradiation and lyophilization on the contents of carotenoids, tissue structure and bacterial counts of carrot. *Journal of the Food Hygienic Society of Japan*, 37(6): 395-400.

Ni, H., and Datta, A. K. (2002). Moisture as related to heating uniformity in microwave processing of solids foods. *Journal of Food Process Engineering*, 22, 367–382.

Ni, H., Datta, A. K., and Torrance, K. E. (1999). Moisture transport in intensive microwave heating of biomaterials: A multiphase porous media model. *International Journal of Heat and Mass Transfer*, 42, 1501–1512.

Nowak D, Levicki PP. 2004. Infrared drying of apple slices. *Innov Food Sci Emerg Technol*. 5:353–60.

Ohlsson T., Bengtsson N., 2002. Minimal processing of foods with thermal methods. In: *Minimal processing technologies in the food industry* (edited by Ohlsson T., Bengtsson N.). Woodhead Publishing Limited, Cambridge, England. Pp. 13-14, 23.

Ohlsson, T., and Bengston, N. (1971). Microwave heating profile in foods—A comparison between heating and computer simulation. *Microwave Energy Applied Newsletter*, 6, 3–8.

Pitchai, K., Birla, S. L., Subbiah, J., Jones, D., and Thippareddi, H. (2012). Coupled electromagnetic and heat transfer model for microwave heating in domestic ovens. *Journal of Food Engineering*, 112, 100–111.

Pitchai, K. (2015). A Finite Element Method Based Microwave Heat Transfer Modeling of Frozen Multi-Component Foods. PhD Thesis. Faculty of The Graduate College at the University of Nebraska

Ranjan, R., Irudayaraj, J., Jun, S., 2002. Simulation of infrared drying process. *Drying Technology*, 20, 363-379.

Ratti, C., & Mujumdar, A. S. (2007). Infrared Drying. In A. S. Mujumdar, *Handbook of Industrial Drying* (pp. 423-438). Boca Raton: CRC Press.

Ren, G., and Chen, F. (1998). Drying of American ginseng *Panax quinquefolium* roots by microwave-hot air combination. *Journal of Food Engineering*, 35, 433±443.

Sahin, S., Sumnu, S. G. (2006). *Physical Properties of Foods*. New York: Springer.

Sakai N, Hanzawa T. 1994. Applications and advances in far-infrared heating in Japan. *Trends Food Sci Technol* 5:357–62.

Salagnac, P., Glouannec, P. and Lecharpentier, D., (2004). Numerical modeling of heat and mass transfer in porous medium during combined hot air, infrared and microwaves drying. *International Journal of Heat and Mass Transfer*, 47, 4479–4489.

Sawai J, Nakai T, Hashimoto A, Shimizu M. 2004. A comparison of the hydrolysis of sweet potato starch with b-amylase and infrared radiation allows prediction of reducing sugar production. *Int J Food Sci Technol* 39:967–74.

Sepulveda, D. R., and G. V. Barbosa-Canovas. 2003. Heat transfer in food products. In *Transport Phenomena in Food Processing*, Eds. J. Welti-Chanes, J. F. Velez-Ruiz, and G. V. Barbosa-Canovas, 42. Boca Raton, FL: CRC Press.

Sharma GP, Verma RC, Pathare PB. 2005. Thin-layer infrared radiation drying of onion slices. *J Food Eng* 67:361–6.

Shilton, N., Mallikarjunan, P., Sheridan, P., 2002. Modeling of heat transfer and evaporative mass losses during the cooking of beef patties using far-infrared radiation. *Journal of Food Engineering* 55 (3), 217–222.

Shivhare, U. S., Raghavan, G. S. V., Bosisio, R. G., & Mujumdar, A. S. (1992). Microwave drying of corn 3. Constant power, intermittent operation. *Transactions of the ASAE*, 35(3), 959–962.

Silva, F. A., Marsaioli, A., Jr., Maximo, G. J., Silva, M. A. A. P., and Goncalves, L. A. G. (2006). Microwave assisted drying of macadamia nuts. *Journal of Food Engineering*, 77, 550–558.

Singh A., Verma S., (2009) “Fundamentals Of Microwave Engineering Principles, Waveguides, Microwave Amplifiers and Applications”. PHI Learning Private Limited, New Delhi.

Sipahioglu, O., & Barringer, S.A. (2003). Dielectric properties of vegetables and fruits as a function of temperature, ash and moisture content. *Journal of Food Science*, 68, 234–239.

Sumnu, G., Turabi, E., & Oztop, M. (2005). Drying of carrots in microwave and halogen lamp–microwave combination ovens. *LWT-Food Science and Technology*, 38:549-553.

Swami, S. (1982). Microwave heating characteristics of simulated high moisture foods. MS Thesis, University of Massachusetts, Amherst, MA.

Tavakolipour H., Mokhtarian M., And Kalbasi-Ashtari A. (2014). Intelligent Monitoring Of Zucchini Drying Process Based On Fuzzy Expert Engine And Ann *Journal of Food Process Engineering* 37 474–481

Terres H. Lizardi A., López R., Morales J.; Lara A. (2014) Experimental Determination Of Convection Heat Transfer Coefficient For Eggplant, Zucchini And Potato Using A Solar Cooker Box-Type. 10th International Conference on Heat Transfer, Fluid Mechanics and Thermodynamics 14 – 16 July 2014 Orlando, Florida

Tireki, S., Sumnu, G., Esin, A., 2006a. Production of bread crumbs by infrared assisted microwave drying, *European Food Research and Technology*, 222, 8-14.

Tireki S, Sumnu G, Esin A (2006b) Effect of microwave, infrared and infrared-assisted microwave heating on the drying rate of bread dough. *Am J Food Technol* 1:82 – 93

Togrul H. 2005. Simple modeling of infrared drying of fresh apple slices. *J Food Eng* 71:311–23.

Tong, C. H. (1988). Microwave heating of baked dough products with simultaneous heat and moisture transfer. PhD thesis, University of Wisconsin, Madison, WI.

Tulasidas, T. N., Raghavan, G. S. V., and Norris, E. R. (1996). Effects of dipping and washing pre-treatments on microwave drying of grapes. *Journal of Food Process Engineering*, 19, 15-25.

Turner J.R., I.W.; Puiggali and W. Jomaa. (1998) A numerical investigation of combined microwave and convective drying of a hygroscopic porous material: a study based on pine wood. *Trans IChemE*, 76 (part A):193

Von Hippel, A. R. (1954). *Dielectrics and Waves*. MIT Press, Cambridge, MA.

W.J. Alton, Society of Manufacturing Engineers, Paper N °. EM98-211, 22 p. (1998).

Wang, J. and Sheng, K., 2006. Far-infrared and microwave drying of peach. *LWT – Food Science and Technology*, 39 (3), 247-255.

Wang, J., and Sheng, K. C. (2004). Modeling of multi-layer far-infrared dryer. *Drying Technology*, 22, 809–820.

Wang, J. and Y. S. Xi. 2005. Drying characteristics and drying quality of carrot using a two-stage microwave process. *Journal of Food Engineering* 68(4): 505-511.

Wei, C. K., Davis, H. T., Davis, E. A. and Gordon, J. (1985). Heat and mass transfer in water-laden sandstone: microwave heating. *AZChE J.*, 31 (5), 842-8.

Yang, H.W., Gunasekaran, S., 2004. Comparison of temperature distribution in model food cylinders based on Maxwell's equations and Lambert's law during pulsed microwave heating. *Journal of Food Engineering* 64 (4), 445–453.

Yongsawatdigul, J., and Gunasekaran, S. (1996). Microwave-vacuum drying of cranberries: Part I. Energy use and efficiency. *Journal of Food Processing and Preservation*, 20(2), 121–144.

Zhou, L., Puri, V. M., Anantheswaran, R. C., and Yeh, G. (1995). Finite element modelling of heat and mass transfer in food materials during microwave heating-model, development and validation. *Journal of Food Engineering*, 25, 509–529.

CURRICULUM VITAE

Name Surname: **Nalan (UYSAL) YAZICIOĞLU**

Nationality: Turkish

Date & Place of Birth: 07/09/1983, İdil, Turkey

Phone: +90 505 467 1107

e-mail: nalan.yazicioglu@gmail.com

EDUCATION

Degree	Institution	Year of Graduation
Ph.D.	M.E.T.U., Food Engineering, Ankara	2016
M.S. M.E.T.U.,	M.E.T.U., Food Engineering, Ankara	2009
B.S. M.E.T.U.,	M.E.T.U., Food Engineering, Ankara	2006
High School	Aydın Super Lisesi	2001

WORK EXPERIENCE

Year	Place	Enrollment
2012-present	Tobacco and Alcohol Market Regulatory Authority, TAPDK, Ankara	Engineer
2006-2012	M.E.T.U., Department of Food Engineering, Ankara	Research Assistant

FOREIGN LANGUAGES

English: Advanced, Italian: Beginner

THESES

Uysal, Nalan, Optimization of Microwave-Infrared Combination Roasting of Hazelnuts, Master of Science Thesis, Middle East Technical University (2009).

PUBLICATIONS

Uysal, N., Sumnu, G., Sahin, S., 2009, Optimization of Microwave-Infrared Roasting of Hazelnut, *Journal of Food Engineering*, 90, 2, 255-261.

Uysal, N., Sumnu, G., Sahin, S., Optimization of Microwave- Convective Heating Combination Roasting of Hazelnuts, International Microwave Power Institute (IMPI) 43rd Annual Symposium July 8-10, 2009 Washington, D. C., USA

I Demirkesen, G Sumnu, S Sahin, N Uysal, Optimisation of formulations and infrared–microwave combination baking conditions of chestnut–rice breads. *International Journal of Food Science & Technology* 46 (9), 1809-1815